0090-9556/07/3502-209–214$20.00
DRUG METABOLISM AND DISPOSITION

DMD 35:209–214, 2007

Vol. 35, No. 2
12567/3169331
Printed in U.S.A.

Involvement of Breast Cancer Resistance Protein (BCRP/*ABCG2*) in the Biliary Excretion and Intestinal Efflux of Troglitazone Sulfate, the Major Metabolite of Troglitazone with a Cholestatic Effect

Junichi Enokizono, Hiroyuki Kusuhara, and Yuichi Sugiyama

Graduate School of Pharmaceutical Sciences, University of Tokyo, Tokyo, Japan

Received August 27, 2006; accepted November 1, 2006

ABSTRACT:

Troglitazone sulfate (TGZS) is the major metabolite of troglitazone (TGZ), an antidiabetic agent, and thought to be a cause of the cholestasis induced by TGZ. The aim of the present study is to elucidate the involvement of breast cancer resistance protein (BCRP/*ABCG2*) in the hepatic disposition of TGZS. The basal-to-apical transport of TGZS was enhanced in organic anion transporting polypeptide 1B1-expressing Madin-Darby canine kidney II cells by infection of recombinant adenovirus harboring human BCRP and mouse Bcrp cDNA. TGZS was given to wild-type and Bcrp (−/−) mice by constant infusion. Biliary excretion is the predominant elimination pathway of TGZS in wild-type mice, and the biliary excretion clearance of TGZS with regard to the hepatic concentration was reduced to 30% of the control in Bcrp (−/−) mice. However, plasma and hepatic concentrations were unchanged, suggesting induction of compensatory mechanisms in Bcrp (−/−) mice for the elimination of TGZS. Involvement of BCRP in the intestinal efflux transport of TGZS was examined using everted sacs. The mucosal efflux clearance of TGZS showed only a slight reduction (15% reduction) in Bcrp (−/−) mice. Our results suggest that BCRP plays a major role in the biliary excretion but a minor role in the intestinal transport of TGZS.

Troglitazone (TGZ) (Fig. 1a) was the first marketed thiazolidinedione, and it has been used for the treatment of type 2 hyperglycemia. It can sensitize tissues to insulin by activating peroxisome proliferator-activated receptor-γ, thereby inhibiting glucose release from hepatocytes and enhancing the insulin-dependent glucose metabolism in adipose tissue and skeletal muscle (reviewed in Chen, 1998). However, TGZ was withdrawn from the market in 2000 because of idiosyncratic severe hepatotoxicity. A great deal of research was carried out on the hepatotoxicity of TGZ, and multiple mechanisms were proposed, such as the production of reactive intermediates and direct mitochondrial injury (reviewed in Smith, 2003). An alternative mechanism that has been proposed is cholestasis. Cholestasis was observed in patients with severe hepatotoxicity (Fukano et al., 2000; Menon et al., 2001), and Funk et al. (2001b) showed that a single bolus administration of TGZ increased the plasma bile acid concentration in rats. Because troglitazone sulfate (TGZS) (Fig. 1b), the major metabolite of TGZ, is a more potent inhibitor of the bile salt export pump (BSEP) than TGZ, and the hepatic concentration of TGZS was much greater than that of TGZ (Funk et al., 2001b), TGZS has been hypothesized to account for the cholestatic effect of TGZ. A gender difference in the cholestatic effect of TGZ in rats was related to the sex-dependent formation of TGZS: the formation of TGZS was greater in male rats, which exhibit more severe cholestasis (Funk et al., 2001a). Based on these findings, it has been speculated that TGZS increases the likelihood of hepatotoxicity induced by TGZ. In addition to the conjugation rate, the hepatic elimination mechanism of TGZS will be important for hepatotoxicity. Elucidation of the molecular mechanism of the hepatic disposition of TGZS is also important to obtain a clue to account for the idiosyncratic hepatotoxicity of TGZ. Polymorphisms or mutations of the enzymes and transporters may be associated with this idiosyncrasy.

TGZS is produced mainly by sulfotransferase (SULT) 1A1 in the liver and is predominantly excreted into the bile (Kawai et al., 1997; Honma et al., 2002). Almost 50% was recovered in the bile as unchanged form after intraduodenum administration of TGZS in rats (Kawai et al., 2000). As far as hepatic uptake is concerned, Nozawa et al. (2004) showed that TGZS is transported by organic anion transporting polypeptide (OATP) 1B1 and OATP1B3, and OATP1B1 transported TGZS more efficiently than OATP1B3 (Nozawa et al., 2004). OATP1B1 will play a major role in the hepatic uptake of TGZS. As far as the biliary excretion process is concerned, Kostrubsky et al. (2001) investigated the involvement of multidrug resistance-

This study was supported by Health and Labour Sciences Research Grants for Research on Regulatory Science of Pharmaceuticals and Medical Devices from Ministry of Health, Labour, and Welfare for the Research on Advanced Medical Technology.

Article, publication date, and citation information can be found at http://dmd.aspetjournals.org.

doi:10.1124/dmd.106.012567.

ABBREVIATIONS: TGZ, troglitazone; TGZS, troglitazone sulfate; BSEP, bile salt excrete pump; SULT, sulfotransferase; OATP, organic anion transporting polypeptide; MRP2/Mrp2, multidrug resistance-associated protein 2; BCRP/Bcrp, breast cancer resistance protein; ME3277, sodium hydrogen {4-[(4,5,6,7-tetrahydrothieno {3,2-c} pyridin-2-yl) carbonylamino] acetyl-o-phenylene} dioxydiacetate; MDCKII, Madin-Darby canine kidney II; GFP, green fluorescent protein; mBcrp, mouse Bcrp; hBCRP, human BCRP; PBS, phosphate-buffered saline; LC/MS, liquid chromatography/mass spectrometry; BSA-KRB, bovine serum albumin/Krebs-Ringer bicarbonate; SNP, single nucleotide polymorphism(s).

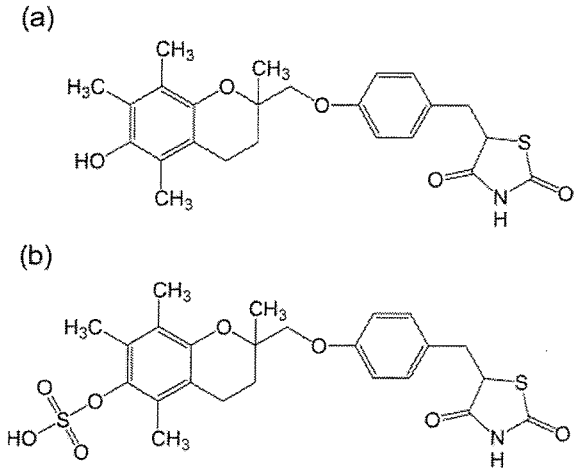

FIG. 1. Chemical structures of TGZ (A) and TGZS (B).

associated protein 2 (MRP2/*ABCC2*) in the biliary excretion of TGZS using TR^- rats, a mutant strain with an inherited deficiency in MRP2. The biliary excretion of TGZS was delayed in TR^- rats compared with normal rats; however, the amount of TGZS excreted into the bile was not markedly reduced in TR^- rats (Kostrubsky et al., 2001). One explanation of this is that other transporters are also involved in the biliary excretion of TGZS. The transport system involved in the intestinal reabsorption of TGZS remains to be identified.

Breast cancer resistance protein (BCRP/*ABCG2*) is a member of the ATP-binding cassette transporter family. BCRP is ubiquitously expressed in normal tissues, and cumulative studies using Bcrp (−/−) mice have shown the importance of BCRP in the urinary excretion, secretion into milk and tissue, and fetal distribution of xenobiotics (Maliepaard et al., 2001; Jonker et al., 2002, 2005). In the liver and intestine, BCRP is localized in the canalicular and brush-border membranes, respectively, and it mediates the biliary excretion of nitrofurantoin and pitavastatin and limits the oral absorption of topotecan, 2-amino-1-methyl-6-phenylimidazo[4,5-b]pyridine, and ME3277 (Jonker et al., 2002; van Herwaarden et al., 2003; Hirano et al., 2005; Kondo et al., 2005; Merino et al., 2005). The substrate specificity of BCRP is characterized by the acceptance of a variety of sulfate conjugates (Suzuki et al., 2003), and BCRP plays a significant role in the efflux transport of certain kinds of sulfate conjugates in the small intestine and kidney (Mizuno et al., 2004; Adachi et al., 2005). Therefore, we hypothesized that BCRP plays a critical role in the prevention of TGZ-induced cholestasis by facilitating biliary excretion, and investigated the contribution of BCRP to the biliary and intestinal excretion of TGZS using Bcrp (−/−) mice.

Materials and Methods

Materials and Animals. TGZ and TGZS were gifts from Sankyo Co. Ltd. (Tokyo, Japan). All the other chemicals were commercially available and of reagent grade. A 24-well Transwell (6.5-mm diameter, 0.4-μm pore size) was purchased from Corning Costar (Bodenheim, Germany). Male Bcrp (−/−) mice (Jonker et al., 2002) and wild-type FVB mice used in the present study were 9 to 16 weeks old and weighed 25 to 33 g. The animals were maintained under controlled temperature with a light/dark cycle of 12 h. Food and water were available ad libitum.

Transcellular Transport Study. The transcellular transport study was performed as previously reported with minor modifications (Matsushima et al., 2005). In brief, Madin-Darby canine kidney II (MDCKII) cells expressing human OATP1B1 (MDCKII/OATP1B1) were grown on the Transwell membrane for 3 days in Dulbecco's modified Eagle's medium (Invitrogen, Carlsbad, CA) with 10% fetal bovine serum (Sigma-Aldrich, St. Louis, MO) and 1% antibiotic-antimycotic solution (Sigma-Aldrich). The cells were infected with the recombinant adenovirus harboring green fluorescent protein (GFP), mouse Bcrp (mBcrp), or human BCRP (hBCRP) expression vector at an infection multiplicity of 200. The details of the construction of these recombinant adenoviruses were described in a previous report (Kondo et al., 2004). After 2 days of culture, the cells were used for transport studies. The cells were preincubated in Krebs-Henseleit buffer (142 mM NaCl, 23.8 mM Na_2CO_3, 4.83 mM KCl, 0.96 mM KH_2PO_4, 1.20 mM $MgSO_4$, 12.5 mM HEPES, 5 mM glucose, and 1.53 mM $CaCl_2$, pH 7.4) for 30 min, and then transport experiments were initiated by replacing the medium on one side of the cell monolayer with Krebs-Henseleit buffer containing 3 μM TGZS. At appropriate times (1, 2, and 3 h), 100-μl aliquots were taken from the opposite side of the cell monolayer and replaced with 100 μl of buffer. After the last sampling, the cell monolayers were solubilized with 500 μl of 0.2 M NaOH and then neutralized with 100 μl of 1 M HCl. The protein concentration was measured by the Lowry method.

The flux of TGZS across cell monolayers was calculated as follows: Flux (μl/mg protein) = ($C_{acceptor}$× $V_{acceptor}$)/(C_{donor}× protein amount), where $C_{acceptor}$ is the TGZS concentration in the acceptor solution, $V_{acceptor}$ is the volume of the acceptor solution, and C_{donor} is the initial TGZS concentration in the donor solution (3 μM). The flux was plotted against time, and the efflux clearances (μl/h/mg protein) were calculated from the slopes.

Determination of Biliary Excretion of TGZS in Wild-Type and Bcrp (−/−) Mice. Under urethane anesthesia (1.25 g/kg, i.p.), the right jugular vein was cannulated with a polyethylene tube (PE-10; Becton Dickinson, Franklin Lakes, NJ) for injection of TGZS. After abdominal dissection, the gallbladder was ligated, and the bile duct was cannulated with a polyethylene tube (UT-3; Unique Medical, Tokyo, Japan) to collect bile. TGZS was injected at a dose of 0.5 μmol/kg, followed by continuous infusion at a dose rate of 0.1 μmol/h/kg. Blood samples were collected from the left jugular vein at 60, 80, 100, and 120 min. The blood samples were heparinized and centrifuged to obtain plasma samples. Bile samples were collected at 20-min intervals between 60 and 120 min postdosing. Immediately after the last blood and bile sampling, mice were sacrificed, and the liver was removed. The liver was homogenized with a 9-fold volume of phosphate-buffered saline (PBS) to obtain a 10% liver homogenate.

The plasma samples (5 μl) were mixed with 20 μl of PBS and 75 μl of acetonitrile; the bile samples (1 μl) were mixed with 49 μl of PBS and 100 μl of acetonitrile; and the liver homogenates (10 μl) were mixed with 40 μl of PBS and 100 μl of acetonitrile. All these mixed solutions were centrifuged at 15,000*g* for 10 min. The supernatants (plasma sample, 80 μl; bile and liver sample, 10 μl) were evaporated, and the pellets were reconstituted with 20% acetonitrile (plasma sample, 80 μl; bile and liver sample, 200 μl) and subjected to liquid chromatography/mass spectrometry (LC/MS) analysis.

Determination of Urinary Excretion of TGZS in Wild-Type and Bcrp (−/−) Mice. Under urethane anesthesia (1.25 g/kg, i.p.), the right jugular vein was cannulated with a polyethylene tube (PE-10) for injection of TGZS, and the urinary bladder was cannulated with two polyethylene tubes (PE-50; Becton Dickinson). One cannula was fitted with a syringe filled with saline to wash the inside of the urinary bladder, and the other cannula was used for the collection of urine and wash solution. TGZS was injected at a dose of 0.5 μmol/kg followed by continuous infusion at a dose rate of 0.1 μmol/h/kg. Mannitol was concomitantly infused at a dose rate of 160 mg/h/kg to increase the urine volume. Urine samples were collected at 20-min intervals between 60 and 120 min. After every collection of urine, the bladder was flushed with about 300 μl of saline, and the wash solution was added to the urine. The urine samples (50 μl) were mixed with 150 μl of acetonitrile and centrifuged at 15,000*g* for 10 min. The supernatants (100 μl) were evaporated, and the pellets were reconstituted in 20% acetonitrile (100 μl) and subjected to LC/MS analysis.

Everted Sac Study. Mice were anesthetized with ether and sacrificed by exsanguination from the femoral artery and vein. Immediately after sacrifice, the ileum was dissected. The ileum was ligated at one end and then everted. The open end of the everted ileum was ligated after the insertion of a polyethylene tube (SP-45; Natsume, Tokyo, Japan) to make a 5-cm-long sac. Krebs-Ringer buffer (350 μl) containing 0.3% bovine serum albumin (BSA-KRB, pH 6.4) was added to the serosal side of the everted sac via the cannula, and the everted sacs were incubated at 37°C in 10 ml of BSA-KRB. After a 10-min preincubation, the everted sacs were placed in BSA-KRB containing

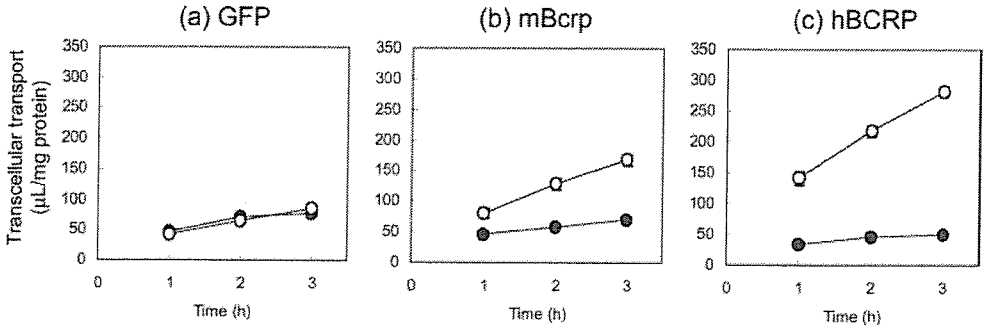

FIG. 2. The transcellular transport of TGZS across monolayers of MDCKII/OATP1B1 expressing GFP, mBcrp, and hBCRP. The transport in the apical-to-basal direction is represented by closed circles and that in the basal-to-apical direction by open circles. Data are represented by mean values ± S.E. of triplicate experiments.

10 μM TGZ and incubated again at 37°C. Aliquots (200 μl) were collected from the mucosal side at 15, 30, 45, and 60 min after incubation with TGZ. After the last sampling, the serosal solution was removed, and the everted sacs were rinsed with ice-cold PBS. Throughout the entire procedure, the mucosal solution was bubbled with O_2/CO_2 (95:5) gas.

The aliquots (75 μl) from the mucosal solution were mixed with acetonitrile (75 μl) and centrifuged at 15,000*g* for 10 min. The supernatants were subjected to LC/MS analysis. The tissue samples were weighed and homogenized with a 9-fold volume of PBS to give 10% tissue homogenates. The tissue homogenates (50 μl) were mixed with acetonitrile (75 μl) and centrifuged at 15,000*g* for 10 min, and the supernatants were subjected to LC/MS analysis.

LC/MS Analysis. An LC/MS-2010 EV equipped with a Prominence LC system (Shimadzu, Kyoto, Japan) was used for the analysis. Samples were separated on a CAPCELL PAK C18 MGII column (3 μm, 2 × 50 mm; Shiseido, Tokyo, Japan) in binary gradient mode. For the mobile phase, 10 mM acetic ammonium and acetonitrile were used. The acetonitrile concentration was initially 23%, then linearly increased up to 70% over 1.5 min, and kept at 70% for a further 1 min. Finally, the column was re-equilibrated at an acetonitrile concentration of 23% for 2.5 min. The total run time was 5 min. TGZS was eluted at 3 min using this method. In the mass analysis, TGZS was detected at a mass-to-charge ratio of 520 under negative electron spray ionization conditions. The interface voltage was −3.5 kV, and the nebulizer gas (N_2) flow was 1.5 l/min. The heat block and curved desolvation line temperatures were 200 and 150°C, respectively.

Data Analysis of Biliary Excretion. Because the plasma and biliary excretion was almost constant between 60 and 120 min (Fig. 3), the plasma and liver concentrations at 120 min were assumed to be steady-state concentrations. Total clearance (CL_{tot}) was calculated by dividing the infusion rate by the plasma concentration at 120 min. The biliary excretion clearance based on the plasma concentration ($CL_{bile,\ plasma}$) was calculated by dividing the biliary excretion rate in the last time segment (100–120 min) by the plasma concentration at 120 min. The biliary excretion clearance based on the liver concentration ($CL_{bile,\ liver}$) was calculated by dividing the biliary excretion rate in the last time segment by the liver concentration at 120 min. The fraction of the biliary excretion was calculated by dividing the biliary excretion rate in the last time segment by the infusion rate.

Efflux Transport in Everted Sac Study. The mucosally excreted amounts of TGZS per unit length of tissue were calculated as follows: Mucosal excretion = ($C_{mucosal} \times V_{mucosal}$)/tissue length, where $C_{mucosal}$ is the TGZS concentration in the mucosal solution, $V_{mucosal}$ is the volume of the mucosal solution (10 ml), and the tissue length was 5 cm. The excreted amounts of TGZS in the mucosal side were plotted against the incubation time (Fig. 4a), and the mucosal efflux rates were estimated from the slope. Mucosal efflux clearances ($CL_{mucosal}$) were calculated by dividing the mucosal efflux rates by the tissue concentrations assuming that 1 g of intestine = 1 ml.

Statistical Analysis. Statistical analysis for significant differences was performed using the two-tailed Student's *t* test or one-way analysis of variance, followed by the Tukey multiple comparison test. A probability of <0.05 was considered to be statistically significant.

Results

In Vitro Transport Study of TGZS in BCRP-Expressed Cells. BCRP-mediated transport of TGZS was examined using GFP-, mBcrp-, and hBCRP-expressed MDCKII/OATP1B1 cells. Figure 2 shows the time courses of the transcellular transport of TGZS in GFP-, mBcrp-, and hBCRP-expressed cell systems. The transport of TGZS increased linearly up to 3 h, suggesting that the initial rates were maintained up to the end of the experiments. The transport rates are summarized in Table 1. The apical-to-basal transport was significantly reduced in hBCRP-expressed cells compared with that in GFP cells. The basal-to-apical transport was significantly increased in both mBcrp- and hBCRP-expressed cells. The ratios of basal-to-apical/apical-to-basal flux were 3.6 and 9.3 in MDCK II cells expressing OATP1B1/mBcrp and OATP1B1/hBCRP, respectively, whereas that in GFP-expressed cells was almost symmetric (flux ratio was 1.45).

TABLE 1

Kinetic parameters of the transcellular transport of TGZS across the monolayers of MDCKII/OATP1B1 cells expressing GFP, mBcrp, and hBCRP

The data are represented by mean values ± S.E. of triplicate experiments. Statistical significance was analyzed by one-way analysis of variance followed by Tukey multiple comparison test.

	Efflux Clearance		Flux Ratio (Basal-to-Apical/ Apical-to-Basal)
	Apical-to-Basal	Basal-to-Apical	
	μl/h/mg protein		
GFP	15.1 ± 0.2	21.9 ± 0.8	1.45 ± 0.06
mBcrp	12.2 ± 3.9	43.9 ± 1.2***	3.60 ± 1.15
hBCRP	7.57 ± 1.01**	70.5 ± 2.8***,†††	9.31 ± 1.30

** $P < 0.01$ and *** $P < 0.001$ statistical differences in efflux clearances with those in GFP-expressed cells.
††† $P < 0.001$ statistical difference in efflux clearances between mBcrp- and hBCRP-expressed cells.

Effect of BCRP on the Biliary Excretion of TGZS. The biliary excretion study was performed by continuous infusion with a priming dose to achieve steady-state conditions. The biliary excretion, plasma, and liver concentrations of TGZS are shown in Fig. 3. The bile flow was almost the same in wild-type and Bcrp (−/−) mice (38.5 ± 4.6 versus 41.8 ± 5.4 μl/min/kg). The plasma concentrations and the biliary excretion of TGZS became almost constant between 60 and 120 min. The plasma concentrations showed a slight reduction in Bcrp (−/−) mice; however, the differences were not statically significant. The biliary excretion of TGZS was markedly reduced in Bcrp (−/−) mice at all the time periods. There was no significant difference in the liver concentrations between wild-type and Bcrp (−/−) mice. The pharmacokinetic parameters are shown in Table 2. The total clearance was slightly increased in Bcrp (−/−) mice, but this was not statistically significant. The biliary excretion clearances based on the plasma and liver concentrations were markedly reduced in Bcrp (−/−) mice to about 30% of those in wild-type mice. The biliary excretion of TGZS was almost 100% in wild-type mice, whereas that in Bcrp (−/−) mice was 32.6%. These results indicate that there is another elimination process for TGZS in Bcrp (−/−) mice. To investigate this, the urinary excretion of TGZS was examined in Bcrp (−/−) mice. However, TGZS concentrations in all the urine samples were

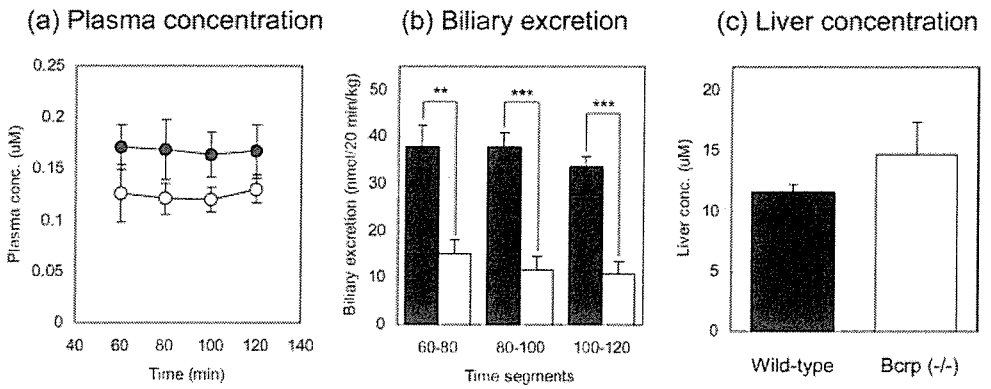

FIG. 3. The effect of BCRP on the biliary excretion of TGZS. a, the time courses of the plasma concentrations of TGZS. b, the biliary excretion of TGZS. c, the liver concentrations of TGZS at 120 min postdosing. The data in wild-type mice are shown by closed circles or columns and those in Bcrp (−/−) mice by open circles or columns. All the data are represented by mean values ± S.E. of four mice. Asterisks represent statistically significant differences between wild-type and Bcrp (−/−) mice; **, $P < 0.01$ and ***, $P < 0.001$.

TABLE 2

Pharmacokinetic parameters of TGZS in the in vivo biliary excretion study

The data are represented by mean values ± S.E. of four mice.

Animal	CL_{total}	$CL_{bile,\ plasma}$	$CL_{bile,\ liver}$	Fraction of Biliary Excretion
	ml/min/kg			%
Wild-type	10.6 ± 1.4	10.9 ± 1.9	0.148 ± 0.017	102 ± 6
Bcrp (−/−)	13.3 ± 1.4	4.15 ± 0.86*	0.0424 ± 0.0115**	32.6 ± 7.9***

* $P < 0.05$, ** $P < 0.01$, and *** $P < 0.001$ statistical significance between wild-type and Bcrp (−/−) mice analyzed by two-tailed Student's t test.

below the lower limit of quantification (10 nM). Because the volume of the urine sample (urine + wash solution) was less than 450 μl at every 20-min period, the urinary excretion rate of TGZS was considered to be less than 0.45 nmol/h/kg. This means that the urinary excretion of TGZS is less than 1% of the dose in Bcrp (−/−) mice.

Effect of BCRP on the Mucosal Efflux Transport of TGZS in Everted Sacs. The effect of BCRP on the mucosal efflux transport of TGZS was examined by using everted ileum sacs. TGZ was added to the mucosal side, and the mucosal efflux of the intracellularly formed TGZS was determined. The results are shown in Fig. 4. The time courses of the mucosal efflux of TGZS were linear, suggesting that the initial rates were maintained up to the end of the experiments. The mucosal efflux was slightly reduced in Bcrp (−/−) mice (Fig. 4a). The tissue concentrations of TGZS at the end of the experiments were similar between wild-type and Bcrp (−/−) mice (Fig. 4b). The mucosal efflux clearance showed a significant but only slight reduction (15.3% decrease) in Bcrp (−/−) mice (Fig. 4c).

Discussion

The present study is focused on the involvement of BCRP in the biliary and intestinal excretion of TGZS. We first examined whether TGZS is a substrate of BCRP in vitro using a BCRP-expressed MDCKII/OATP1B1 system where OATP1B1 and BCRP are localized in the basal and apical membrane, respectively, and the basal-to-apical transport of their common substrates is increased (Matsushima et al., 2005). Compared with GFP-expressed cells, the basal-to-apical transport was increased in mBcrp- and hBCRP-expressed cells, suggesting that TGZS is a substrate of both mBcrp and hBCRP. A higher flux ratio was observed in hBCRP-expressed cells than in mBcrp-expressed cells, suggesting that hBCRP transports TGZS more efficiently than mBcrp.

In the in vivo study, there was no significant difference in bile flow between in wild-type and Bcrp (−/−) mice. The bile flow obtained in the present study was about 40 μl/min/kg and within the range of previously reported bile flows in FVB male mice (28.7 and 61 μl/min/kg) (Wang et al., 2001; Werner et al., 2002). These results suggested that cholestasis was not induced under the present experimental conditions. Funk et al. (2001b) showed the cholestatic effect of TGZ in rats. In that report, the plasma and liver concentrations of TGZS were 110 and 260 μM, respectively, much higher than those in the present study (plasma, 0.1–0.2 μM; liver, 10–15 μM). This suggests that the plasma and liver concentrations of TGZS in the present study were too low to induce cholestasis.

Comparison of the total body and biliary excretion clearances showed that biliary excretion is the main elimination pathway of TGZS in wild-type mice. The biliary excretion of TGZS was markedly reduced in Bcrp (−/−) mice, and $CL_{bile,\ liver}$, which represents the intrinsic efflux ability at the canalicular membrane, was reduced in Bcrp (−/−) mice to 29% of that in wild-type mice. Therefore, BCRP is the major transporter involved in the biliary excretion of TGZS. Cumulative studies using Mrp2-deficient mutant rats have shown that MRP2 accounts for the biliary excretion of some sulfate conjugates, such as tauro-conjugated bile acid sulfate, phenolphthalein sulfate, and acetaminophen sulfate (Takikawa et al., 1991; Akimoto et al., 2001; Tanaka et al., 2003; Zamek-Gliszczynski et al., 2005). Very recently, Zamek-Gliszczynski et al. (2006) showed that BCRP is also involved in the biliary excretion of sulfate conjugates, including 4-methylumbelliferone sulfate, acetaminophen sulfate, and harmol sulfate, using Bcrp (−/−) mice. These results suggest that BCRP and MRP2 are two major transporters responsible for the biliary excretion of sulfate conjugates, and BCRP makes a major contribution to the biliary excretion of xenobiotic sulfate conjugates. In humans, the biliary excretion of TGZS may be mediated by BCRP because hBCRP transports TGZS more efficiently than mBcrp.

The total clearance and hepatic concentration were not changed in Bcrp (−/−) mice, although biliary excretion is the predominant elimination pathway in wild-type mice. At steady state, the biliary excretion accounts for, at most, 30% of the total body clearance in Bcrp (−/−) mice, and the remaining fraction could be explained by other elimination mechanisms that were induced to compensate for the loss of biliary excretion. Urinary excretion could be an alternative elimination pathway of TGZS. However, the urinary excretion of TGZS was negligible in Bcrp (−/−) mice. Therefore, induction of hepatic metabolic enzymes is a likely mechanism. Currently, there is no information regarding the enzymes that are induced in Bcrp (−/−) mice, and further studies are necessary to identify them.

The effect of BCRP on the intestinal reabsorption was examined using everted ileum sacs. The mucosal efflux clearance ($CL_{mucosal}$) of TGZS represents the intrinsic efflux ability of TGZS in the brush-border membrane of the intestinal epithelial cells, and the effect of BCRP on the mucosal excretion of TGZS can be measured by a comparison of $CL_{mucosal}$ between wild-type and Bcrp (−/−) mice. The $CL_{mucosal}$ of TGZS showed only a slight reduction in Bcrp (−/−)

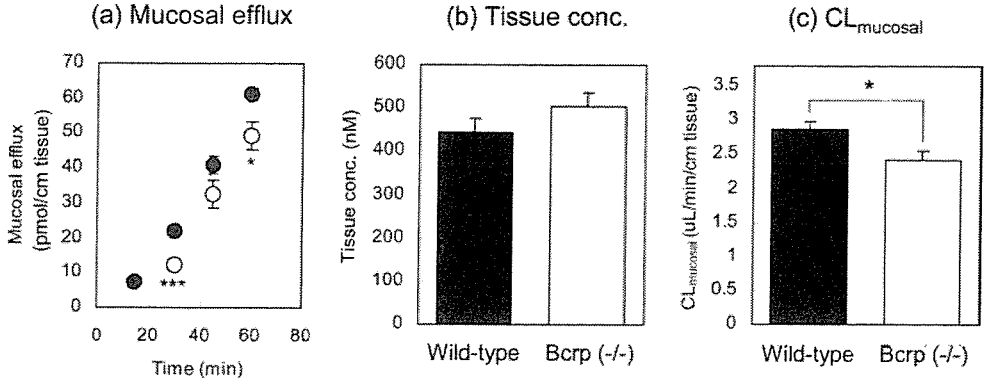

FIG. 4. The effect of BCRP on the intestinal transport of TGZS in everted ileum sacs. a, the time courses of the mucosal efflux of TGZS. b, the tissue concentrations of TGZS after a 60-min incubation. c, the mucosal efflux clearances of TGZS. The data in wild-type mice are shown by closed circles or columns and those in Bcrp (−/−) mice by open circles or columns. All the data are represented by mean values ± S.E. of four everted sacs independently prepared from four mice. Asterisks represent statically significant differences between wild-type and Bcrp (−/−) mice; *, $P < 0.05$ and ***, $P < 0.001$.

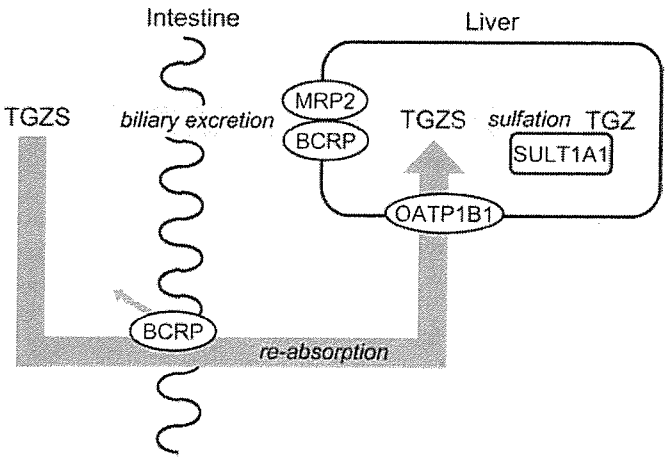

FIG. 5. Schematic representation of the molecular mechanism involved in the hepatic disposition of TGZS.

mice. This result suggests that BCRP plays only a limited role in preventing oral absorption of TGZS.

Figure 5 summarizes the molecular mechanism involved in the hepatic disposition of TGZS. TGZS is produced by SULT1A1 from TGZ and is excreted into the bile mainly by BCRP. TGZS excreted into the intestinal lumen undergoes reabsorption into the circulating blood (Kawai et al., 2000). SULT1A1, BCRP, and OATP1B1 are the important molecules controlling the hepatic disposition of TGZS. BCRP has some functional single nucleotide polymorphisms (SNP), such as C376T (Q126stop), C421A (Q141K), and G1322A (S441N). The C376T mutation introduces a stop codon, resulting in the production of truncated BCRP (Imai et al., 2002). The C421A allele is associated with a reduction in the protein level (Imai et al., 2002; Kondo et al., 2004; Kobayashi et al., 2005). The G1322A allele affects both the protein level and localization of BCRP (Kondo et al., 2004). Among these SNP, C421A exhibits the highest frequency (about 10 and 30% in Caucasian and Japanese, respectively) (Kobayashi et al., 2005). Clinical studies revealed that the plasma exposure of diflomotecan, topotecan, and rosuvastatin was higher in subjects carrying the C421A allele (Sparreboom et al., 2004, 2005; Zhang et al., 2006). These functional SNP of BCRP may increase the liver and/or plasma exposure of TGZS, affecting the susceptibility to TGZS if any induction of compensatory mechanisms, which were observed in Bcrp (−/−) mice but do not occur in humans. Besides BCRP, SULT1A1 and OATP1B1 also have functional SNP (Raftogianis et al., 1997; Nowell et al., 2002; Nishizato et al., 2003; Mwinyi et al., 2004; Wegman et al., 2005; Maeda et al., 2006). A combination of these functional SNP in BCRP, SULT1A1, and OATP1B1 may be involved in the idiosyncratic hepatotoxicity of TGZ.

In conclusion, our present study revealed that TGZS is a substrate of mBcrp and hBCRP and that the biliary excretion of TGZS is mainly mediated by BCRP in mice.

Acknowledgments. We thank Sankyo Co. Ltd. for supplying us with TGZ and TGZS, Dr. Kazuya Maeda and Soichiro Matsushima for providing MDCK cells expressing OATP1B1, and Dr. Alfred H. Schinkel (The Netherlands Cancer Institute, The Netherlands) for supplying Bcrp (−/−) mice.

References

Adachi Y, Suzuki H, Schinkel AH, and Sugiyama Y (2005) Role of breast cancer resistance protein (Bcrp1/Abcg2) in the extrusion of glucuronide and sulfate conjugates from enterocytes to intestinal lumen. *Mol Pharmacol* **67**:923–928.

Akimoto K, Sano N, and Takikawa H (2001) Biliary excretion of tauroursodeoxycholate-3-sulfate in the rat. *Steroids* **66**:701–705.

Chen C (1998) Troglitazone: an antidiabetic agent. *Am J Health Syst Pharm* **55**:905–925.

Fukano M, Amano S, Sato J, Yamamoto K, Adachi H, Okabe H, Fujiyama Y, and Bamba T (2000) Subacute hepatic failure associated with a new antidiabetic agent, troglitazone: a case report with autopsy examination. *Hum Pathol* **31**:250–253.

Funk C, Pantze M, Jehle L, Ponelle C, Scheuermann G, Lazendic M, and Gasser R (2001a) Troglitazone-induced intrahepatic cholestasis by an interference with the hepatobiliary export of bile acids in male and female rats. Correlation with the gender difference in troglitazone sulfate formation and the inhibition of the canalicular bile salt export pump (Bsep) by troglitazone and troglitazone sulfate. *Toxicology* **167**:83–98.

Funk C, Ponelle C, Scheuermann G, and Pantze M (2001b) Cholestatic potential of troglitazone as a possible factor contributing to troglitazone-induced hepatotoxicity: in vivo and in vitro interaction at the canalicular bile salt export pump (Bsep) in the rat. *Mol Pharmacol* **59**:627–635.

Hirano M, Maeda K, Matsushima S, Nozaki Y, Kusuhara H, and Sugiyama Y (2005) Involvement of BCRP (ABCG2) in the biliary excretion of pitavastatin. *Mol Pharmacol* **68**:800–807.

Honma W, Shimada M, Sasano H, Ozawa S, Miyata M, Nagata K, Ikeda T, and Yamazoe Y (2002) Phenol sulfotransferase, ST1A3, as the main enzyme catalyzing sulfation of troglitazone in human liver. *Drug Metab Dispos* **30**:944–949.

Imai Y, Nakane M, Kage K, Tsukahara S, Ishikawa E, Tsuruo T, Miki Y, and Sugimoto Y (2002) C421A polymorphism in the human breast cancer resistance protein gene is associated with low expression of Q141K protein and low-level drug resistance. *Mol Cancer Ther* **1**:611–616.

Jonker JW, Buitelaar M, Wagenaar E, Van Der Valk MA, Scheffer GL, Scheper RJ, Plosch T, Kuipers F, Elferink RP, Rosing H, et al. (2002) The breast cancer resistance protein protects against a major chlorophyll-derived dietary phototoxin and protoporphyria. *Proc Natl Acad Sci USA* **99**:15649–15654.

Jonker JW, Merino G, Musters S, van Herwaarden AE, Bolscher E, Wagenaar E, Mesman E, Dale TC, and Schinkel AH (2005) The breast cancer resistance protein BCRP (ABCG2) concentrates drugs and carcinogenic xenotoxins into milk. *Nat Med* **11**:127–129.

Kawai K, Hirota T, Muramatsu S, Tsuruta F, Ikeda T, Kobashi K, and Nakamura KI (2000) Intestinal absorption and excretion of troglitazone sulphate, a major biliary metabolite of troglitazone. *Xenobiotica* **30**:707–715.

Kawai K, Kawasaki-Tokui Y, Odaka T, Tsuruta F, Kazui M, Iwabuchi H, Nakamura T, Kinoshita T, Ikeda T, Yoshioka T, et al. (1997) Disposition and metabolism of the new oral antidiabetic drug troglitazone in rats, mice and dogs. *Arzneimittelforschung* **47**:356–368.

Kobayashi D, Ieiri I, Hirota T, Takane H, Maegawa S, Kigawa J, Suzuki H, Nanba E, Oshimura M, Terakawa N, et al. (2005) Functional assessment of ABCG2 (BCRP) gene polymorphisms to protein expression in human placenta. *Drug Metab Dispos* **33**:94–101.

Kondo C, Onuki R, Kusuhara H, Suzuki H, Suzuki M, Okudaira N, Kojima M, Ishiwata K, Jonker JW, and Sugiyama Y (2005) Lack of improvement of oral absorption of ME3277 by prodrug formation is ascribed to the intestinal efflux mediated by breast cancer resistant protein (BCRP/ABCG2). *Pharm Res (NY)* **22**:613–618.

Kondo C, Suzuki H, Itoda M, Ozawa S, Sawada J, Kobayashi D, Ieiri I, Mine K, Ohtsubo K, and Sugiyama Y (2004) Functional analysis of SNPs variants of BCRP/ABCG2. *Pharm Res (NY)* **21**:1895–1903.

Kostrubsky VE, Vore M, Kindt E, Burliegh J, Rogers K, Peter G, Altrogge D, and Sinz MW

(2001) The effect of troglitazone biliary excretion on metabolite distribution and cholestasis in transporter-deficient rats. *Drug Metab Dispos* **29**:1561–1566.
Maeda K, Ieiri I, Yasuda K, Fujino A, Fujiwara H, Otsubo K, Hirano M, Watanabe T, Kitamura Y, Kusuhara H, et al. (2006) Effects of organic anion transporting polypeptide 1B1 haplotype on pharmacokinetics of pravastatin, valsartan, and temocapril. *Clin Pharmacol Ther* **79**:427–439.
Maliepaard M, Scheffer GL, Faneyte IF, van Gastelen MA, Pijnenborg AC, Schinkel AH, van De Vijver MJ, Scheper RJ, and Schellens JH (2001) Subcellular localization and distribution of the breast cancer resistance protein transporter in normal human tissues. *Cancer Res* **61**:3458–3464.
Matsushima S, Maeda K, Kondo C, Hirano M, Sasaki M, Suzuki H, and Sugiyama Y (2005) Identification of the Hepatic efflux transporters of organic anions using double-transfected madin-darby canine kidney II cells expressing human organic anion-transporting polypeptide 1B1 (OATP1B1)/multidrug resistance-associated protein 2, OATP1B1/multidrug resistance 1, and OATP1B1/breast cancer resistance protein. *J Pharmacol Exp Ther* **314**:1059–1067.
Menon KVN, Angulo P, and Lindor KD (2001) Severe cholestatic hepatitis from troglitazone in a patient with nonalcoholic steatohepatitis and diabetes mellitus. *Am J Gastroenterol* **96**:1631–1634.
Merino G, Jonker JW, Wagenaar E, van Herwaarden AE, and Schinkel AH (2005) The breast cancer resistance protein (BCRP/ABCG2) affects pharmacokinetics, hepatobiliary excretion, and milk secretion of the antibiotic nitrofurantoin. *Mol Pharmacol* **67**:1758–1764.
Mizuno N, Suzuki M, Kusuhara H, Suzuki H, Takeuchi K, Niwa T, Jonker JW, and Sugiyama Y (2004) Impaired renal excretion of 6-hydroxy-5,7-dimethyl-2-methylamino-4-(3-pyridylmethyl) benzothiazole (E3040) sulfate in breast cancer resistance protein (BCRP1/ABCG2) knockout mice. *Drug Metab Dispos* **32**:898–901.
Mwinyi J, Johne A, Bauer S, Roots I, and Gerloff T (2004) Evidence for inverse effects of OATP-C (SLC21A6) 5 and 1b haplotypes on pravastatin kinetics. *Clin Pharmacol Ther* **75**:415–421.
Nishizato Y, Ieiri I, Suzuki H, Kimura M, Kawabata K, Hirota T, Takane H, Irie S, Kusuhara H, Urasaki Y, et al. (2003) Polymorphisms of OATP-C (SLC21A6) and OAT3 (SLC22A8) genes: consequences for pravastatin pharmacokinetics. *Clin Pharmacol Ther* **73**:554–565.
Nowell S, Sweeney C, Winters M, Stone A, Lang NP, Hutchins LF, Kadlubar FF, and Ambrosone CB (2002) Association between sulfotransferase 1A1 genotype and survival of breast cancer patients receiving tamoxifen therapy. *J Natl Cancer Inst* **94**:1635–1640.
Nozawa T, Sugiura S, Nakajima M, Goto A, Yokoi T, Nezu J, Tsuji A, and Tamai I (2004) Involvement of organic anion transporting polypeptides in the transport of troglitazone sulfate: implications for understanding troglitazone hepatotoxicity. *Drug Metab Dispos* **32**:291–294.
Ott P, Ranek L, and Young MA (1998) Pharmacokinetics of troglitazone, a PPAR-gamma agonist, in patients with hepatic insufficiency. *Eur J Clin Pharmacol* **54**:567–571.
Raftogianis RB, Wood TC, Otterness DM, Van Loon JA, and Weinshilboum RM (1997) Phenol sulfotransferase pharmacogenetics in humans: association of common SULT1A1 alleles with TS PST phenotype. *Biochem Biophys Res Commun* **239**:298–304.
Smith MT (2003) Mechanisms of troglitazone hepatotoxicity. *Chem Res Toxicol* **16**:679–687.
Sparreboom A, Gelderblom H, Marsh S, Ahluwalia R, Obach R, Principe P, Twelves C, Verweij J, and McLeod HL (2004) Diflomotecan pharmacokinetics in relation to ABCG2 421C>A genotype. *Clin Pharmacol Ther* **76**:38–44.
Sparreboom A, Loos WJ, Burger H, Sissung TM, Verweij J, Figg WD, Nooter K, and Gelderblom H (2005) Effect of ABCG2 genotype on the oral bioavailability of topotecan. *Cancer Biol Ther* **4**:650–658.
Suzuki M, Suzuki H, Sugimoto Y, and Sugiyama Y (2003) ABCG2 transports sulfated conjugates of steroids and xenobiotics. *J Biol Chem* **278**:22644–22649.
Takikawa H, Sano N, Narita T, Uchida Y, Yamanaka M, Horie T, Mikami T, and Tagaya O (1991) Biliary excretion of bile acid conjugates in a hyperbilirubinemic mutant Sprague-Dawley rat. *Hepatology* **14**:352–360.
Tanaka H, Sano N, and Takikawa H (2003) Biliary excretion of phenolphthalein sulfate in rats. *Pharmacology* **68**:177–182.
van Herwaarden AE, Jonker JW, Wagenaar E, Brinkhuis RF, Schellens JH, Beijnen JH, and Schinkel AH (2003) The breast cancer resistance protein (Bcrp1/Abcg2) restricts exposure to the dietary carcinogen 2-amino-1-methyl-6-phenylimidazo[4,5-b]pyridine. *Cancer Res* **63**:6447–6452.
Wang DQ, Paigen B, and Carey MC (2001) Genetic factors at the enterocyte level account for variations in intestinal cholesterol absorption efficiency among inbred stains of mice. *J Lipid Res* **42**:1820–1830.
Wegman P, Vainikka L, Stal O, Nordenskjold B, Skoog L, Rutqvist LE, and Wingren S (2005) Genotype of metabolic enzymes and the benefit of tamoxifen in postmenopausal breast cancer patients. *Breast Cancer Res* **7**:R284–R290.
Werner A, Minich DM, Havinga R, Bloks V, Van Goor H, Kulipers F, and Verkade HJ (2002) Fat malabsorption in essential fatty acid-deficient mice is not due to impaired bile formation. *Am J Physiol* **283**:G900–G908.
Zamek-Gliszczynski MJ, Hoffmaster KA, Tian X, Zhao R, Polli JW, Humphreys JE, Webster LO, Bridges AS, Kalvass JC, and Brouwer KL (2005) Multiple mechanisms are involved in the biliary excretion of acetaminophen sulfate in the rat: role of Mrp2 and Bcrp1. *Drug Metab Dispos* **33**:1158–1165.
Zamek-Gliszczynski MJ, Nezasa K, Tian X, Kalvass JC, Patel NJ, Raub TJ, and Brouwer KL (2006) The important role of Bcrp (Abcg2) in the biliary excretion of sulfate and glucuronide metabolites of acetaminophen, 4-methylumbelliferone, and harmol in mice. *Mol Pharmacol* **70**:2127–2133.
Zhang W, Yu BN, He YJ, Fan L, Li Q, Liu ZQ, Wang A, Liu YL, Tan ZR, Fen J, et al. (2006) Role of BCRP 421C>A polymorphism on rosuvastatin pharmacokinetics in healthy Chinese males. *Clin Chim Acta* **373**:99–103.

Address correspondence to: Yuichi Sugiyama, Graduate School of Pharmaceutical Sciences, The University of Tokyo, 7-3-1, Hongo, Bunkyo-ku, Tokyo 113-0033, Japan. E-mail: sugiyama@mol.f.u-tokyo.ac.jp

EUROPEAN JOURNAL OF PHARMACEUTICAL SCIENCES 27 (2006) 425–446

available at www.sciencedirect.com

SCIENCE DIRECT

journal homepage: www.elsevier.com/locate/ejps

PHARMACEUTICAL SCIENCES

Review

Transporters as a determinant of drug clearance and tissue distribution

Yoshihisa Shitara[a], *Toshiharu Horie*[a], *Yuichi Sugiyama*[b,*]

[a] *Department of Biopharmaceutics, Graduate School of Pharmaceutical Sciences, Chiba University, 1-8-1, Inohana, Chou-ku, Chiba 260-8675, Japan*

[b] *Department of Molecular Pharmacokinetics, Graduate School of Pharmaceutical Sciences, The University of Tokyo, 7-3-1, Hongo, Bunkyo-ku, Tokyo 113-0033, Japan*

ARTICLE INFO

Article history:
Received 26 October 2005
Received in revised form 1 December 2005
Accepted 6 December 2005

Keywords:
Transporter
Drug elimination
Pharmacokinetics

ABSTRACT

Transporters play an important role in the processes of drug absorption, distribution and excretion. In this review, we have focused on the involvement of transporters in drug excretion in the liver and kidney. The rate of transporter-mediated uptake and efflux determines the rate of renal and hepatobiliary elimination. Transporters are thus important as a determinant of the clearance in the body. Even when drugs ultimately undergo metabolism, their elimination rate is sometimes determined by the uptake rate mediated by transporters. Transporters regulate the pharmacological and/or toxicological effect of drugs because they limit their distribution to tissues responsible for their effect and/or toxicity. For example, the liver-specific distribution of some statins via organic anion transporters helps them to produce their high pharmacological effect. On the other hand, as in the case of metformin taken up by organic cation transporter 1, drug distribution to the tissue(s) may enhance its toxicity. As transporter-mediated uptake is a determinant of the drug elimination rate, drug–drug interactions involving the process of transporter-mediated uptake can occur. In this review, we have introduced some examples and described their mechanisms.

More recently, some methods to analyze such transporter-mediated transport have been reported. The estimation of the contributions of transporters to the net clearance of a drug makes it possible to predict the net clearance from data involving drug transport in transporter-expressing cells. Double transfected cells, where both uptake and efflux transporters are expressed on the same polarized cells, are also helpful for the analysis of the rate of transporter-mediated transcellular transport.

Contents

1. Introduction 426
2. Hepatic and renal transporters as a determinant of drug disposition 428
   2.1. Substrates of hepatobiliary transporters 428
   2.2. Involvement of hepatic uptake transporters in the drug disposition 429

* *Corresponding author*. Tel.: +81 3 5841 4770; fax: +81 3 5800 6949.
E-mail address: sugiyama@mol.f.u-tokyo.ac.jp (Y. Sugiyama).

0928-0987/$ – see front matter © 2005 Elsevier B.V. All rights reserved.
doi:10.1016/j.ejps.2005.12.003

2.2.1. Transporters can be a rate-limiting factor in the elimination of drugs 429
2.2.2. Transporters determine the tissue distribution of drugs 430
2.3. Substrates of renal transporters 432
2.4. The balance of hepatic and renal clearances determine the elimination pathway 432
3. The mechanism of transporter-mediated drug–drug interactions 435
4. A method for estimating the contribution of each transporter to the total hepatic uptake 437
4.1. The importance of the contribution of transporters 437
4.2. Estimation of the contributions of specific transporters to the total hepatic uptake 437
5. Transport studies using double transfected cells 440
6. Conclusion 441
References 441

1. Introduction

Drug elimination in the liver consists of the following processes: (1) hepatic uptake, (2) metabolism and/or (3) biliary excretion (Pang and Rowland, 1977; Pang and Gillette, 1978; Yamazaki et al., 1996a; Shitara et al., 2005). In addition, (4) sinusoidal efflux from the inside of the cell to the blood also determine the hepatic elimination rate. Among these processes, drug transporters are involved in uptake, sinusoidal efflux and biliary excretion (Meier et al., 1997; Kullak-Ublick et al., 2000; van Montfoort et al., 2003; Giacomini and Sugiyama, 2005). Recently, molecular cloning of drug transporters has greatly helped the characterization of the mechanism of drug elimination in the liver (Hagenbuch and Meier, 2003; Keppler and Konig, 2000; Mizuno et al., 2003). It should be noted that hepatic uptake and biliary excretion determine the drug concentration in the liver, and they may affect the pharmacological effects and/or toxic side effects (Giacomini and Sugiyama, 2005). Thus, drug transporters are also a determinant of pharmacological effects and/or side effects for drugs whose target is the liver.

In the kidney, drug clearances are determined by: (1) glomerular filtration, (2) tubular secretion and (3) reabsorption (Inui et al., 2000a,b; Dresser et al., 2001). As glomerular filtration is simply the ultrafiltration of drugs not bound to plasma proteins, no transporters are involved. Transporters are mainly involved in tubular secretion and reabsorption (Koepsell and Endou, 2004; Sekine et al., 2000; Wright and Dantzler, 2004). Several active transport mechanisms have been reported in the proximal tubules and these are involved in secretion. Reabsorption is sometimes mediated by transporters although many drugs are reabsorbed only by passive

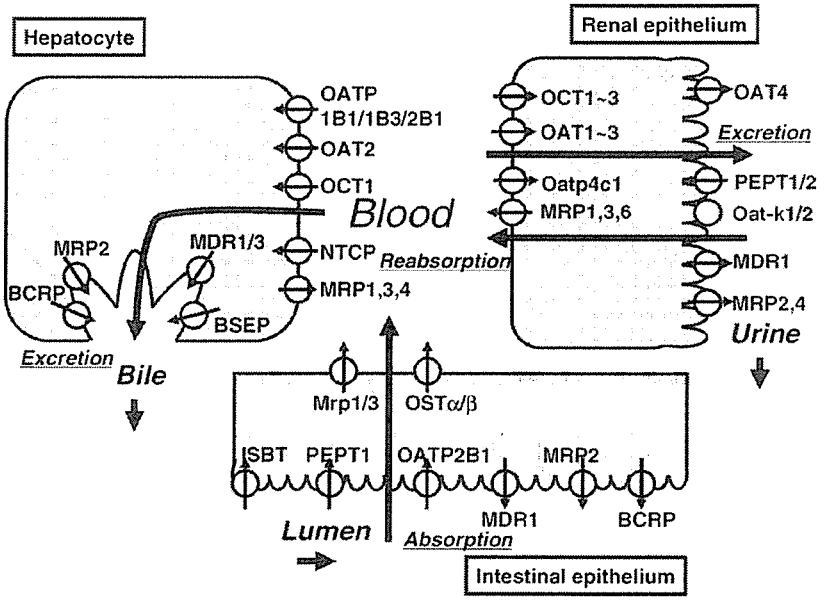

Fig. 1 – Transporters involved in the intestinal absorption, hepatic excretion and renal excretion of drugs. Multiple transporters are involved in the transcellular transport of drugs in the liver, kidney and intestine. For transcellular transport, drugs need to cross two different membranes on the basal and apical sides. In the intestine, drugs are absorbed from the luminal side (brush border membrane) and excreted into the portal blood across the basolateral membrane. In the liver, drugs are taken up into hepatocytes across the sinusoidal membrane and excreted into the bile. In the kidney, drugs undergo secretion (urinary excretion) or reabsorption. In the case of secretion, drugs are taken up from the basolateral side and excreted in the urine across the apical side. However, in the case of reabsorption, drugs are taken up from the urine and excreted in the circulating blood.

diffusion depending on a high drug concentration gradient across the blood and nephron, which is caused by reabsorption of water back into the plasma.

Orally administered drugs firstly pass through the intestine and subsequently appear in the portal blood. This intestinal absorption affects the drug concentration in the circulating blood. Moreover, the intestine functions as a barrier to xenobiotics (Wacher et al., 2001; Zhang and Benet, 2001). In these processes, transporters in intestine play important roles (Ganapathy and Leibach, 1982; Amidon and Lee,

Table 1 – Therapeutic drugs which are substrates of hepatic transporters

		Uptake transporters	Metabolizing enzymes	Bile canalicular tranporters	References
Atorvastatin	Human	OATP1B1	CYP3A4		Kameyama et al. (2005) Lau et al. (2006)
Bosentan	Human		CYP2C9 CYP3A4		
	Rat	Oatp1a1 Oatp1a4 Oatp1b2			Treiber et al. (2004)
Caspofungin	Human	OATP1B1	–		Sandhu et al. (2005)
Cerivastatin	Human	OATP1B1	CYP3A4 CYP2C8		Shitara et al. (2003)
	Rat	Oatp1a1 Oatp1a4 Oatp1b2			Shitara et al. (2004b)
Fexofenadine	Human	OATP1B1[a] OATP1B3 OATP2B1[b]	–	MDR1	Cvetkovic et al. (1999) Niemi et al. (2005a) Shimizu et al. (2005)
	Rat	Oatp1a1 Oatp1a4	–		Cvetkovic et al. (1999)
Glycyrrhizin[c]	Human	OATP1B1 OATP1B3			Ismair et al. (2003)
	Rat	Oatp1a1 Oatp1a4 Oatp1b2			Ismair et al. (2003)
Pravastatin	Human	OATP1B1 OATP2B1	– –	MRP2 BSEP BSEP BCRP MDR1	 Hsiang et al. (1999) Nakai et al. (2001) Sasaki et al. (2002) Kobayashi et al. (2003) Nozawa et al. (2004) Hirono et al. (2005) Matsushima et al. (2005)
	Rat	Oatp1a1 Oatp1a4 Oatp1b2	–	Mrp2	Hsiang et al. (1999) Tokui et al. (1999) Sasaki et al. (2004)
Pitavastatin	Human	OATP1B1 OATP1B3[b]	CYP2C9*	MRP2 BCRP MDR1	Hirano et al. (2004, 2005a, 2005b)
Rifampicin	Human	OATP1B1 OATP1B3		MDR1	Schuetz et al. (1996) Vavricka et al. (2002) Tirona et al. (2003)
Repaglinide	Human	OATP1B1	CYP2C8 CYP3A4		Niemi et al. (2005b)
Rosuvastatin	Human	OATP1B1 OATP1B3 OATP2B1	–	MRP2 MDR1 BCRP	Schneck et al. (2004) Kitamura et al. (2005) Huang et al., in press
Telmisartan	Human	OATP1B3	UGTs	MRP2 (as a glucuronide)	Nishino et al. (2000) Ishiguro et al. (2005)

[a] The pharmacokinetics of fexofenadine was altered in subjects with genetic polymorphism of OATP1B1. But the involvement of OATP1B1 in the hepatic uptake of fexofenadine has not been shown directly.
[b] Minor contribution.
[c] Glycyrrhizin is reported only as an inhibitor of uptake transporters.

1994; Tsuji and Tamai, 1996; Terada and Inui, 2004). Transporters in the liver, kidney and intestine are illustrated in Fig. 1.

Transporters in other tissues are also determinants of the distribution of drugs to the target organs for the pharmacological effects and/or adverse reactions. Since the distribution volume of drugs to the brain is generally low, transporters in the brain do not affect the plasma concentration of drugs. However, they control the drug distribution to the brain, affecting the pharmacological effects or side effects (Tamai and Tsuji, 2000; Kusuhara and Sugiyama, 2004, 2005).

In this manuscript, we shall focus on the transporter functions in the kidney and liver and review the mechanisms of drug elimination. We will also describe a recently developed method of analyzing transporter function by estimating the contribution of each transporter, and the use of transporter double transfectants.

2. Hepatic and renal transporters as a determinant of drug disposition

2.1. *Substrates of hepatobiliary transporters*

Table 1 shows some of therapeutic drugs which are substrates of transporters in the liver. Among them, some drugs are taken up into hepatocytes, followed by metabolism while others are excreted into the bile in intact form (Stieger and Meier, 1998; Keppler and Konig, 2000; van Montfoort et al., 2003; Fujino et al., 2004a). For example, atorvastatin, a 3-hydroxy-3-methyglutaryl coenzyme A (HMG-CoA) reductase inhibitor (statin), is taken up into liver via transporter(s) including organic anion transporting polypeptide 1B1 (OATP1B1/OATP-C/OATP2/LST-1, gene symbol; *SLCO1B1/SLC21A6*), subsequently undergoing metabolism by cytochrome P450 3A4 (CYP3A4) (Lennernas, 2003; Kameyama et al., 2005; Lau et al., 2006). In the case of cerivastatin, CYP2C8 and 3A4 are responsible for its metabolism after its hepatic uptake (Muck, 2000; Shitara et al., 2003, 2004a). On the other hand, pravastatin and rosuvastatin are reported to be mainly excreted in intact form (Hatanaka, 2000; White, 2002). Although pitavastatin is metabolized by CYP2C9, the metabolic rate is very low (Fujino et al., 2004b). In fact, it is excreted into bile mainly in the intact form in experimental animals including rats, rabbits and dogs (Kojima et al., 1999). Table 1 also shows the elimination pathway following the hepatic uptake. For some of the drugs listed in Table 1, the hepatic extraction ratio and the fraction excreted into urine as the unchanged form is shown in Table 2. In this table, the hepatic extraction ratio is calculated by the hepatic clearance, which is the total body clearance minus the renal clearance, divided by the hepatic blood flow.

The hepatobiliary transport mechanism of pravastatin has been studied in rats. Its Michaelis constant (K_m) determined in vitro for hepatic uptake is 29–37 μM while that for biliary excretion is 220 μM (Yamazaki et al., 1993, 1997; Ishigami et al., 1995). On the other hand, the K_m value for the hepatic elimination rate in vivo is close to that for the hepatic uptake process in vitro, suggesting that the rate-limiting step for the overall hepatic elimination in rats is the uptake (Yamazaki et al., 1996b).

Table 2 – Hepatic extraction of substrate drugs of hepatic uptake transporter(s)

	CL_{tot} (L/h)	f_e	E_H
Cerivastatin	13	0	0.13
Pravastatin	57	0.47	0.31
Rosuvastatin	49	0.30	0.36
Repaglinide	38	0.080	0.36
Valsartan	2.2	0.29	0.016
Bosentan	13	<0.01	0.14

f_e: fraction excreted in urine as an unchanged form; E_H: hepatic extraction ratio, E_H was calculated based on the following equation: $E_H = CL_H/Q_H$ where, CL_H is hepatic clearance, that is total body clearance minus renal clearance, and Q_H is hepatic blood flow rate (96.6 L/h).

In rats, Oatp1a1 (Oatp1, *Slco1a1/Slc21a1*), Oatp1a4 (Oatp2, *Slco1a4/Slc21a5*) and Oatp1b2 (Oatp4, *Slco1b2/Slc21a10*) are involved in the hepatic uptake of pravastatin (Hsiang et al., 1999; Tokui et al., 1999; Sasaki et al., 2004). Among them, there are conflicting reports of the involvement of Oatp1a4: Hsiang et al. showed that Oatp1a4 does not accept pravastatin as a substrate while Tokui et al. described its saturable transport in Oatp1a4-expressing *Xenopus laevis* oocytes. This discrepancy may be due to the difference in the experimental systems used: i.e. cDNA transfected mammalian cells versus cRNA injected *Xenopus laevis* oocytes. The uptake study in isolated rat hepatocytes showed that most of the hepatic uptake of pravastatin (92–93%) is mediated by a saturable process (Table 3). In humans, OATP1B1 and OATP2B1 (*SLCO2B1/SLC21A9*) accept pravastatin as a substrate among hepatic uptake transporters, and OATP1B1 seems to play a major role (Hsiang et al., 1999; Nakai et al., 2001; Kobayashi et al., 2003; Nozawa et al., 2004). Recent studies using MDCK cells expressing OATP1B1 and efflux transporter (multidrug resistance associated protein 2 (MRP2; *ABCC2*), multidrug resistance 1 (MDR1; *ABCB2*) or breast cancer resistance protein (BCRP; *ABCG2*)) showed that the biliary excretion of pravastatin is mediated by multiple transporters in humans (Sasaki et al., 2002; Matsushima et al., 2005). Not only MRP2 but also BCRP and MDR1 may play roles in its biliary excretion, though the contribution of MRP2 seems to be the highest (Sasaki et al., 2002; Matsushima et al., 2005). Moreover, bile salt export pump (BSEP, *ABCB11*) is also reported to be involved in its biliary excretion (Hirano et al., 2005a). Recent studies indicate that genetic polymorphisms in OATP1B1 alter the pharmacokinetics of pravastatin, suggesting that transporter-mediated hepatic uptake is the main determinant of its plasma clearance (Nishizato et al., 2003; Niemi et al., 2004; Mwinyi et al., 2004). More recently, genetic polymorphism in OATP1B1 was also found to alter the pharmacokinetics of pitavastatin similar to pravastatin (Chung et al., 2005).

Even for drugs, whose clearances are dependent on metabolism, the hepatic uptake can become rate determining in the overall elimination. For cerivastatin, it is clear that the uptake process is the rate-limiting factor in humans and rats in its elimination because cyclosporin A (CsA), which inhibits its transporter-mediated hepatic uptake with mini-

Table 3 – Uptake of drugs into isolated human or rat hepatocytes

	K_m (μM)	V_{max} (pmol/min/mg protein)	V_{max}/K_m (μL/min/mg protein)	P_{dif} (μL/min/mg protein)	References
Human					
Pravastatin	12	10	0.89	0.30	Nakai et al. (2001)
Cerivastatin	180	5200[a]	280[a]	70[a]	Shitara et al. (2003)
	2.6	550[a]	210[a]	65[a]	Shitara et al. (2003)
	3.7	360[a]	97[a]	42[a]	Shitara et al. (2003)
Pitavastatin	3.0	80	27	7.7	Fujino et al. (2004a)
Rat					
Pravastatin	29	550	19	1.6	Yamazaki et al. (1993)
	37	820	22	1.6	Ishigami et al. (1995)
Cerivastatin	5.9	260	44	24	Shitara et al. (2004a)
Pitavastatin	26	3100	120	1.2	Shimada et al. (2003)
Rosuvastatin	9.2	–	–	–	Nezasa et al. (2003)
Glycyrrhizin	11	110[a]	9.9[a]	–	Ishida et al. (1993)
Bumetanide	140	980	6.9	–	Follmann et al. (1990)
Cephalexin	6300	2300	0.36	–	Tamai and Tsuji (1987)
Benzylpenicillin	470	2000	4.3	–	Tsuji et al. (1986)
Glibenclamide	3.1	420	130	–	Petzinger and Fuckel (1992)
Indomethacin	12	1100	93	2.1	Kouzuki et al. (2000)
Grepafloxacin	170	6700	40	28	Sasabe et al. (1997)
Levofloxacin	440	8600	20	14	Sasabe et al. (1997)

[a] Based on per 10^6 cells.

mal effects on metabolism, alters its plasma clearance in vivo (Muck et al., 1999; Shitara et al., 2003, 2004b). Repaglinide, an antidiabetic drug, is also metabolized by CYP2C8 and 3A4 (Bidstrup et al., 2003). Its total clearance is also affected by the genetic polymorphism of OATP1B1, suggesting OATP1B1-mediated uptake is a determinant of its pharmacokinetics (Niemi et al., 2005b) (Fig. 2). More recent studies have shown that CsA alters the pharmacokinetics of repaglinide, supporting that transporter-mediated hepatic uptake is a determinant of its pharmacokinetics (Kajosaari et al., 2005). Bosentan, an endothelin receptor antagonist, is metabolized by CYP2C9 and 3A4 (Dingemanse and van Giersbergen, 2004). Although the mechanism of its hepatic uptake in humans is still to be investigated, its pharmacokinetic behavior in rats is affected by the coadministration of CsA (Treiber et al., 2004) (Fig. 3). Treiber et al. analyzed the mechanism of this pharmacokinetic interaction and concluded that it was mainly due to the inhibition of Oatp-mediated hepatic uptake because the inhibition of Mdr1a/b (*Abcb1a/b*) did not cause a serious alteration in the pharmacokinetics of bosentan and the inhibition of metabolism was insufficient to explain the serious interaction between these two drugs. This pharmacokinetic interaction was also reported in humans in clinical trials, suggesting its pharmacokinetics in humans is also determined by hepatic uptake transporters (Binet et al., 2000) (Fig. 3). Telmisartan, an angiotensin receptor antagonist, is excreted in bile as its glucuronide conjugate, at least partly, via Mrp2 (*Abcc2*) in rats (Nishino et al., 2000). Recently, OATP1B3 (OATP8, *SLCO1B3/SLC21A8*) has been suggested to be involved in the hepatic uptake of telmisartan in humans (Ishiguro et al., 2005). Accordingly, this transporter may be a determinant of the pharmacokinetics of telmisartan. As described here, for some drugs which are taken up into the liver via transporter(s), the uptake can be a limiting process of the elimination rate even when their final elimination pathway is metabolism.

2.2. *Involvement of hepatic uptake transporters in the drug disposition*

2.2.1. *Transporters can be a rate-limiting factor in the elimination of drugs*

Fig. 4(A) shows the scheme of the hepatic elimination of drugs. In this section, the role of transporters in the hepatic uptake and biliary excretion with regard to the overall elimination is presented based on a clearance concept. The overall hepatic intrinsic clearance ($CL_{int,all}$) can be described by the following equation (Pang and Gillette, 1978; Yamazaki et al., 1996a):

$$CL_{int,all} = PS_{u,influx} \times \frac{CL_{int}}{CL_{int} + PS_{u,efflux}} \quad (1)$$

where $PS_{u,influx}$ and $PS_{u,efflux}$ are the membrane permeability–surface area products of unbound drugs across the sinusoidal membrane for the influx and efflux processes, respectively, and CL_{int} is the 'exact' intrinsic clearance for unbound drugs, which includes the metabolism and biliary excretion of unchanged drugs. When the $PS_{u,efflux}$ is negligibly low compared with the CL_{int} ($PS_{u,efflux} \ll CL_{int}$), Eq. (1) can be approximated by the following equation:

$$CL_{int,all} = PS_{u,influx} \quad (2)$$

In this case, the hepatic uptake predominantly determines the net hepatic clearance. On the other hand, when the $PS_{u,efflux}$ is much higher than the CL_{int} ($PS_{u,efflux} \gg CL_{int}$), Eq. (1) can be

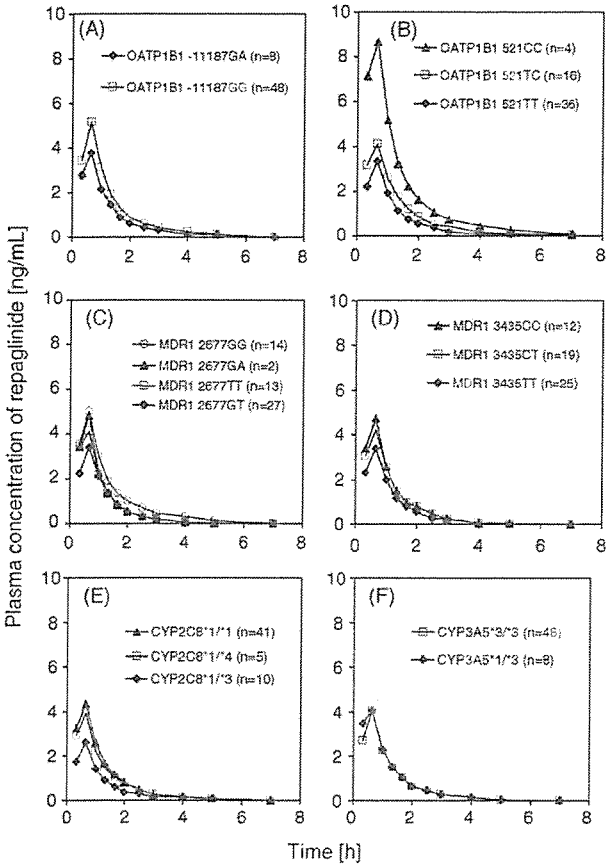

Fig. 2 – Mean plasma concentration of repaglinide in healthy subjects in relation to the single nucleotide polymorphisms in OATP1B1 (A and B) and MDR1 (C and D) and different genotypes in CYP2C8 (E) and CYP3A5 (F). Fifty-six Finnish healthy volunteers were participated in this study and genotyped for the −11187G>A in the promoter region and the 521T>C in exon 5 of the *SLCO1B1* (OATP1B1) gene, the 3435C>T in exon 26 of the *ABCB1* (MDR1) gene, the *CYP2C8*3* and *4 and the *CYP3A4*3* and the mean plasma concentrations of repaglinide after 0.25 mg single oral administration in relation to their genotypes are shown. A statistically significant difference was observed only in the C_{max} and AUC between OATP1B1 (521TT) and (521CC) (Niemi et al., 2005b).

approximated by the following equation:

$$CL_{int,all} = PS_{u,influx} \times \frac{CL_{int}}{PS_{u,efflux}} \quad (3)$$

In this case, all processes shown in Fig. 4(A) affect the net hepatic clearance. When the permeation across the sinusoidal membrane is sufficiently rapid and the transports from the inside of cells to the outside and in the opposite direction are symmetric (i.e. $PS_{u,influx} = PS_{u,efflux}$), Eq. (1) can be approximated by the following equation:

$$CL_{int,all} = CL_{int} \quad (4)$$

In this case, the apparent intrinsic clearance ($CL_{int,all}$) equals the exact intrinsic clearance (CL_{int}). This is applicable to drugs which are lipophilic with rapid membrane permeability. Fig. 4(B) shows the relationship between the apparent $CL_{int,all}$ and 'exact' CL_{int}. When the CL_{int} is low, $CL_{int,all}$ is proportional to CL_{int}. However, when it is high, $CL_{int,all}$ is not affected by CL_{int} and affected only by the uptake clearance, i.e. it is uptake-limited.

Table 4 shows the pharmacokinetic changes in lovastatin, simvastatin and atorvastatin following coadministration of CYP3A4 inhibitors. CYP3A4 inhibitors affect their CL_{int} including the metabolic clearance. Among these statins, lovastatin and simvastatin are lipophilic with lactone ring and are taken up into cells rapidly via passive diffusion while atorvastatin undergoes transporter-mediated uptake (Kameyama et al., 2005; Lau et al., 2006). Following hepatic uptake, they are metabolized in the liver with a minimal excretion in urine as unchanged form. The net hepatic clearance is described by Eq. (1). In the case of lovastatin and simvastatin, which are lipophilic and extensively metabolized by CYP3A4, the net hepatic clearances are close to Eq. (4) (Sirtori, 1993), and their hepatic clearances are directly affected by the change in CL_{int}. On the other hand, the net hepatic clearance of atorvastatin is affected by both metabolism and hepatic uptake (Kameyama et al., 2005; Lau et al., 2006). As atorvastatin is highly taken up into hepatocytes by transporter(s) and well metabolized, its $CL_{int,all}$ is described by Eq. (2) and may be minimally affected by alterations in CL_{int}. In fact, CYP3A4 inhibitors markedly alter the pharmacokinetics of lovastatin and simvastatin, but they have a much weaker effect on that of atorvastatin (Table 4). For example, itraconazole increased the area under the plasma concentration–time curve (AUC) of lovastatin and simvastatin over 10-fold while it increased that of atorvastatin only two- to three-fold (Neuvonen and Jalava, 1996; Neuvonen et al., 1998; Kantola et al., 1998a; Mazzu et al., 2000). Erythromycin increased the AUC of simvastatin acid four-fold although its effect on the AUC of the lactone form of simvastatin is unknown (Kantola et al., 1998b) while it increased that of atorvastatin only 1.3-fold (Siedlik et al., 1999). Nelfinavir, an HIV protease inhibitor, increased the AUC of simvastatin acid six-fold, but that of atorvastatin only 1.7-fold (Hsyu et al., 2001). The combined administration of ritonavir and saquinavir drastically increased the AUC of simvastatin 31-fold while it increased that of atorvastatin 3.5-fold (Fichtenbaum et al., 2002). Grapefruit juice is also known to be a potent inhibitor of CYP3A4 and it increased the AUC of simvastatin and simvastatin acid 3.6- and 3.3-fold, respectively (Lilja et al., 1998). Its effect on the AUC of lovastatin has reported to be marked (2.0- to 15-fold and 1.6- to 5-fold for lovastatin and lovastatin acid, respectively) in two independent reports (Kantola et al., 1998c; Rogers et al., 1999). On the other hand it only produced a minor increase in the AUC of atorvastatin (1.4- to 2.5-fold) (Lilja et al., 1999).

2.2.2. *Transporters determine the tissue distribution of drugs*

Transporters also affect the tissue distribution, and contribute to the selective distribution of drugs to specific tissues. As the pharmacological target of statins is the liver, they should be selectively distributed there. Pravastatin has been reported

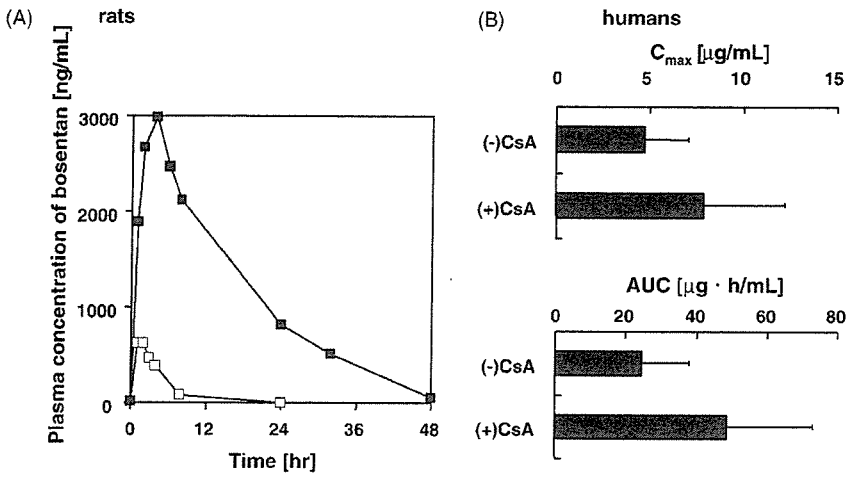

Fig. 3 – Pharmacokinetic alterations of bosentan in rats and humans by coadministration of CsA. (A) Male Wistar rats were orally administered bosentan with (■) or without (□) intraperitoneal administration of CsA. Coadministration of CsA increased the C_{max} and $AUC_{0-\infty}$ of orally administered repaglinide 4.4 and 17 times, respectively. (B) Ten male volunteers were orally given 500 mg bosentan twice daily starting at day 1 in the morning until day 8 and 300 mg CsA (Sandimmun Neoral®) twice daily starting at day 1 in the evening until day 8. The pharmacokinetics of bosentan were evaluated at day 1 ((−)CsA) and day 8 ((+)CsA). The C_{max} and $AUC_{0-\infty}$ of orally administered repaglinide were increased 1.7 and 2.0 times, respectively, by coadministration of CsA ($p = 0.08$ and 0.04 for C_{max} and $AUC_{0-\infty}$, respectively) (Treiber et al., 2004; Binet et al., 2000).

to be a substrate of OATP1B1 and multiple transporters on the bile canalicular membrane, including MRP2 (Sasaki et al., 2002; Matsushima et al., 2005; Hirano et al., 2005b). These transporters assist the liver-specific distribution of pravastatin. Pravastatin is, thus, excreted into the bile, reabsorbed in the intestine to the portal vein and taken up by the liver, and effectively undergoes enterohepatic circulation (Kato et al., 2002). Therefore, the liver concentration should be higher than that in the circulating blood, leading to a high pharmacological effect at a relatively low plasma concentration. Also, in the case of rosuvastatin and pitavastatin, they are effectively and selectively taken up into hepatocytes via OATP1B1 and mainly excreted into bile as the unchanged forms like pravastatin (Fujino et al., 2004b; Simonson et al., 2004). Although atorvastatin is metabolized by CYP3A4, it is also taken up into the liver via OATP1B1, suggesting that it is also effectively dis-

Table 4 – Effect of CYP3A4 inhibitors on the metabolism of simvastatin, lovastatin and atorvastatin

Inhibitor	Substrate	AUC fold increase	C_{max} fold increase	References
Itraconazole	Simvastatin	>10	>10	Neuvonen et al. (1998)
	Simvasatin acid	19	17	Neuvonen et al. (1998)
	Lovastatin	>15–>20	15–>20	Neuvonen and Jalava (1996)
	Lovastatin acid	15	12	Neuvonen and Jalava (1996)
	Atorvastatin	2.5–3	N.S.–1.38	Kantola et al. (1998a), Mazzu et al. (2000)
Erythromycin	Simvastatin acid	3.9	5	Kantola et al. (1998b)
	Atorvastatin	1.3	1.4	Siedlik et al. (1999)
Clarithromycin	Atorvastatin	1.8	1.6	Amsden et al. (2002)
Nelfinavir	Simvastatin acid	6.1	6.2	Hsyu et al. (2001)
	Atorvastatin	1.7	2.2	Hsyu et al. (2001)
Ritonavir + saquinavir	Simvastatin acid	31	31	Fichtenbaum et al. (2002)
	Atorvastatin	3.5	4.3	Fichtenbaum et al. (2002)
Grapefruit juice	Simvastatin	3.6	3.9	Kantola et al. (1998c)
	Simvastatin acid	3.3	4.3	Kantola et al. (1998c)
	Lovastatin	1.9–15	1.7–12	Lilja et al. (1998)
	Lovastatin acid	1.6–5.0	1.7–4	Lilja et al. (1998)
	Atorvastatin	1.4–2.5	1.1	Lilja et al. (1999)

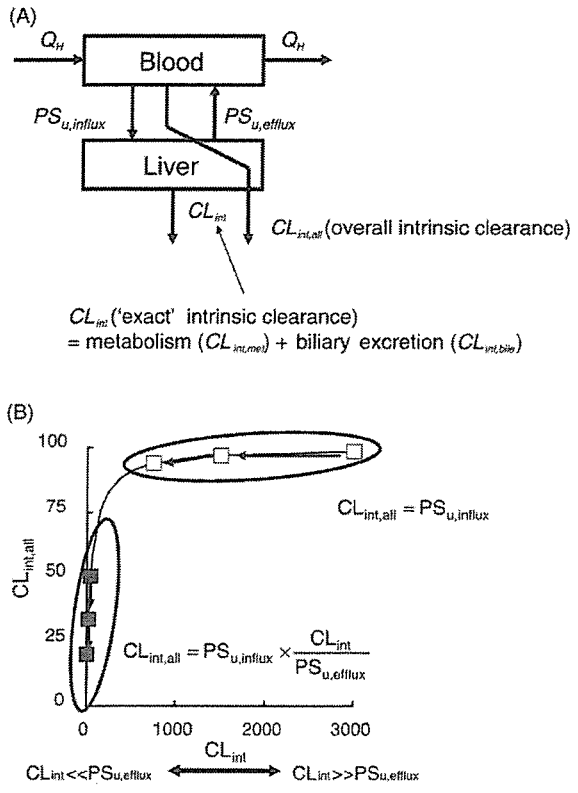

Fig. 4 – The mechanism of the overall hepatic intrinsic clearance of drugs. (A) Drugs that are excreted in the liver are firstly taken up into hepatocytes, followed by metabolism or biliary excretion. At the sinusoidal membrane, transporters can produce back efflux into the blood. Thus, the overall hepatic elimination process includes all these. The overall hepatic intrinsic clearance can be expressed as a hybrid parameter of membrane transport across the sinusoidal membrane from the blood side into hepatocytes (uptake: $PS_{u,influx}$), that from the inside of hepatocytes to the blood side ($PS_{u,efflux}$) and the 'exact' intrinsic clearance (CL_{int}) including drug metabolism and biliary excretion, as described by $CL_{int,all} = PS_{u,influx} \times (CL_{int}/(CL_{int} + PS_{u,efflux}))$ (Eq. (1)). (B) The relation between $CL_{int,all}$ (y-axis) and CL_{int} (x-axis). CL_{int} is higher than the $PS_{u,efflux}$, the overall intrinsic clearance is close to the uptake clearance (uptake-limited). When the intrinsic clearance is quite low, the overall intrinsic clearance can be described by a hybrid parameter of $PS_{u,influx}$, $PS_{u,efflux}$ and CL_{int}. In the case of $CL_{int} \gg PS_{u,influx}$, $CL_{int,all}$ is not affected by the alteration in the CL_{int}. On the other hand, in the case of $CL_{int} \ll PS_{u,influx}$, it depends on the CL_{int}.

tributed to the liver and exert its high pharmacological effect there (Lennernas, 2003; Kameyama et al., 2005; Lau et al., 2006).

Biguanide antidiabetic drugs are taken up into hepatocytes via organic cation transporter 1 (OCT1, *SLC22A1*), but undergoes a minimal metabolism or biliary excretion, mainly resulting in urinary excretion (Wang et al., 2002) (Fig. 5). Wang et al. used Oct1 (*Slc22a1*) knockout mice to show that metformin, a biguanide, is distributed to the liver via Oct1 (Wang et al., 2002). The plasma concentration of metformin was similar in Oct1 (+/+) and (−/−) mice because its elimination is mainly via urinary excretion. However, its liver concentration is affected by Oct1 and it is approximately 30 times lower in Oct1 (−/−) than in Oct1 (+/+). Lactic acidosis is one of the side effects of biguanides and it depends on their liver concentration. In Fig. 6 , the plasma concentration of metformin and lactate in Oct1 (+/+) and (−/−) mice is shown (Wang et al., 2003). The lactate level is markedly different without a difference in the plasma concentration of metformin in Oct1 (+/+) and (−/−). This means that transporters can sometimes affect the pharmacological effects or adverse reactions without any apparent pharmacokinetic alterations.

Rifampicin is well known for its ability to induce drug-metabolizing enzymes and transporters, through activation of the pregnane X receptor (PXR). This activation should be influenced by the concentration of rifampicin in the liver. Thus, hepatic uptake transporters should be a determinant of the induction of enzymes and transporters. Tinora et al. showed that it is a substrate of human OATP1B1, 1B3 and rat Oatp1b2 (Tirona et al., 2003). In humans, OATP1B1 seems to have far greater affinity and capacity for rifampicin transport than OATP1B3. Thus, they suggested that OATP1B1 is a major determinant of rifampin mediated PXR activation. In fact, PXR activation is examined at lower concentration of rifampin in zinc-induced OATP1B1-expressing HeLa cells than in uninduced control cells (Tirona et al., 2003).

2.3. *Substrates of renal transporters*

Transporters are involved in tubular secretion and reabsorption during the renal excretion process (Inui et al., 2000a; Koepsell and Endou, 2004; Shitara et al., 2005). In the kidney, drugs are required to pass through the plasma membranes, the basolateral membrane and the brush border membrane, for transcellular transport. The transporters in the kidney are illustrated in Fig. 1. Table 5 shows a number of drugs which undergo transporter-mediated renal excretion and their urinary excretion ratio as unchanged form. The transporters responsible for their urinary excretion are also shown in Table 5. However, the detailed transport mechanism remains to be investigated for most of drugs because there are few cases where efflux transporters on the brush-border membrane have been characterized.

2.4. *The balance of hepatic and renal clearances determine the elimination pathway*

Drugs are predominantly metabolized or excreted in the urine and bile. Therefore, the total body clearance (CL_{tot}) is a summation of CL_H and renal clearance (CL_R) as described by the following equation:

$$CL_{tot} = CL_R + CL_H \quad (5)$$

This equation shows that the balance of CL_R and CL_H determines the elimination pathway. In addition, CL_R and CL_H are regulated by the affinity and capacity of drugs for transporters in the kidney and liver, respectively. As described in

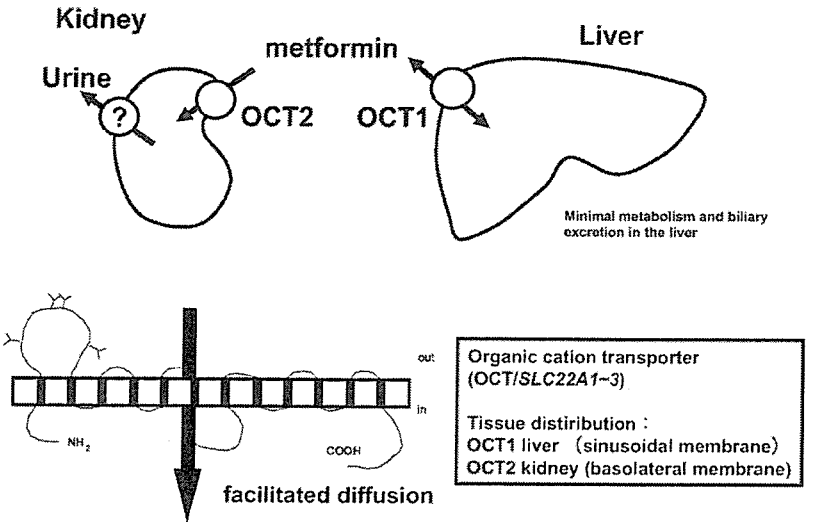

Fig. 5 – The mechanism of tissue distribution of metformin. OCT1 is expressed in the liver while OCT2 is localized on the basolateral membrane in the renal epithelial cells. They transport substrate drugs by a facilitated diffusion. Although metformin is taken up into liver via OCT1, it undergoes a minimal metabolism and biliary excretion. Thus, it mainly undergoes urinary excretion, after renal uptake via OCT2.

Section 2.2, pravastatin is distributed to the liver by hepatic uptake mediated by transporters. On the other hand, its urinary excretion as unchanged form in humans is relatively high (41–47% after intravenous administration) (Hatanaka, 2000). This is attributed to the fact that pravastatin is a substrate of renal transporter(s). Yamazaki et al. studied the renal transport mechanism of pravastatin in rats and showed that its renal uptake is inhibited by *p*-aminohippurate, suggesting the existence of a saturable transport system for it (Yamazaki et al., 1996c). Hasegawa et al. analyzed the molecular mechanism of renal uptake of pravastatin in rats (Hasegawa et al., 2002). They showed that rat organic anion transporter 3 (Oat3; *Slc22a8*) accepts pravastatin as a substrate while Oat1 (*Slc22a6*) does not. The K_m value for its uptake in rat kidney slices was similar with that in rat Oat3-expressing LLC-PK_1 cells. In addition, the inhibition studies of the uptake of pravastatin by *p*-aminohippurate (a relatively selective inhibitor of rat Oat1), benzylpenicillin (a relatively selective inhibitor of rat Oat3) and dibromosulfophthalein (a non-specific inhibitor of rat Oat1 and Oat3) revealed their inhibition constants were similar in rat kidney slices and Oat3-expressing cells. These results suggested that its renal uptake is mediated by Oat3 (Hasegawa et al., 2002). Takeda et al. showed that it is a substrate of human OAT3 (*SLC22A8*) (Takeda et al., 2004). As OAT3 is expressed on the basolateral membrane of kidney proximal tubules, it may help the renal uptake of pravastatin in humans.

The pharmacokinetics of temocaprilat, the active metabolite of temocapril, an angiotensin converting enzyme (ACE) inhibitor, is relatively unaffected by renal failure (Oguchi et al., 1993). This is thought to be due to the fact that temo-

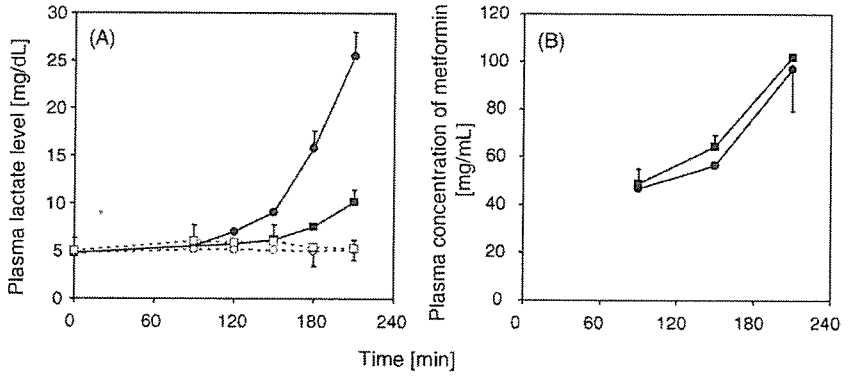

Fig. 6 – Plasma lactate level after metformin administration in Oct1(+/+) and (−/−) mice. The plasma lactate level in Oct1(+/+) (■, □) or (−/−) (●, ○) mice with (■, ●) or without (□, ○) intravenous infusion of metformin at the rate of 150 mg/h/kg (A). Although the plasma concentration of metformin is similar in Oct1(+/+) (■) and (−/−) mice (●) (B), its effect on the plasma lactate level was different. This different lactate level in the plasma is due to the difference in the hepatic uptake of metformin as the target organ for lactic acidosis is the liver. This result suggests the involvement of OCT1 in the lactic acidosis caused by biganides including metformin (Wang et al., 2003).

Table 5 – Urinary excretion ratio of substrate drugs of kidney transporters

	f_e	Involved transporters	References
Acyclovir	0.75	Human OAT1[a]	Takeda et al. (2002a)
		Human OCT1[a]	Takeda et al. (2002a)
		Rat Oat1[a]	Wada et al. (2000)
		Rat Oat3[b]	Ohtsuki et al. (2002)
Adefovir	0.70–0.80	Human OAT1[a]	Cihlar et al. (1999), Ho et al. (2000)
		Rat Oat1[a]	Cihlar et al. (1999)
Cidofovir	0.70	Human OAT1[a]	Cihlar et al. (1999), Ho et al. (2000)
		Rat Oat1[a]	Cihlar et al. (1999)
Amoxicillin	0.86	Human PEPT1[b]	Wenzel et al. (1996)
		Rat Oat1[b]	Jariyawat et al. (1999)
		Rat Pept1[b]	Wenzel et al. (1996), Jariyawat et al. (1999), Terada et al. (1997)
		Rat Pept2[b]	Wenzel et al. (1996), Jariyawat et al. (1999), Terada et al. (1997)
Enalapril	0.88	Human PEPT1[b]	Han et al. (1998), Han et al. (1999)
		Rat Oatp1a1[a]	Pang et al. (1998), Abu-Zahra et al. (2000)
		Rat Pept1[b]	Temple and Boyd (1998)
Temocaprilat	0.090–0.32[c]	Rat Mrp2[a]	Ishizuka et al. (1997)
		Rat Oatp1a1[a]	Ishizuka et al. (1997)
Cefadroxil	0.84	Human OAT1[b]	Takeda et al. (2002b)
		Human OAT3[b]	Takeda et al. (2002b)
		Rat Oat1[b]	Jung et al. (2002)
		Rat Oat3[b]	Jung et al. (2002)
		Human PEPT1[b]	Wenzel et al. (1996), Ganapathy et al. (1995)
		Human PEPT2[b]	Ganapathy et al. (1995)
		Rat Pept1[a]	Terada et al. (1997), Ganapathy et al. (1995)
		Rat Pept2[a]	Terada et al. (1997)
Cefamandole	0.71	Human OAT1[b]	Takeda et al. (2002b)
		Human OAT3[b]	Takeda et al. (2002b)
		Human OAT4[b]	Takeda et al. (2002b)
		Rat Oat1[b]	Jariyawat et al. (1999), Jung et al. (2002)
		Rat Oat3[b]	Jung et al. (2002)
Cefazolin	0.80	Human OAT1[b]	Takeda et al. (2002b)
		Human OAT3[b]	Takeda et al. (2002b)
		Human OAT4[b]	Takeda et al. (2002b)
		Rat Oat1[b]	Jariyawat et al. (1999)
		Rat Oat3[b]	Jung et al. (2002)
Cimetidine	0.62	Human OAT1[a]	Burckhardt et al. (2003)
		Human OAT3[a]	Cha et al. (2001)
		Rat Oat3[a]	Kusuhara et al. (1999)
		Rat Oct1[a]	Grundemann et al. (1999)
Pravastatin	0.47	Human OAT3[a]	Takeda et al. (2004)
		Rat Oat3[a]	Hasegawa et al. (2002)

f_e: Fraction excreted in urine as an unchanged form.

[a] Reported as a substrate.

[b] Reported as an inhibitor.

[c] Excreted as temocaprilat, a prodrug of temocapril.

caprilat undergoes both renal and hepatic elimination. This is a special feature among classic ACE inhibitors, and this is helped by the presence of MRP2/Mrp2 in the bile canalicular membrane of hepatocytes (Ishizuka et al., 1997). Although other classic ACE inhibitors are also taken up into hepatocytes via transporter(s), they are not excreted into the bile so much and are mainly excreted in the urine. On the other hand, temocaprilat is a substrate of MRP2/Mrp2, and excreted in the bile. Therefore, the total clearance of temocaprilat is the sum of the hepatic and renal clearances while that of other ACE inhibitors is mainly due to their renal clearance. Due to this dual elimination pathway, changes in renal function do not affect the plasma concentration of temocaprilat so much. However, other ACE inhibitors are markedly affected by renal failure because they have no other elimination pathways than in the urine. It is, therefore, very necessary to be able to predict the substrate specificity of MRP2 in silico. The authors were recently involved in this in silico prediction (Hirono et al., 2005). In this study, key functional groups of multiple rat Mrp2 ligand molecules were identified, their relative locations were determined and substrate specificity of rat Mrp2 was examined using the three-dimensional quantitative

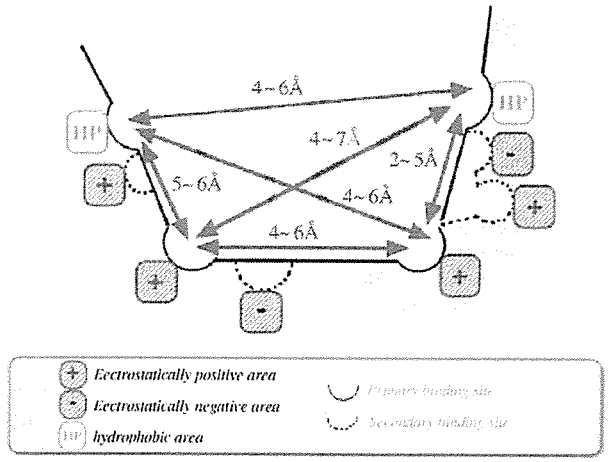

Fig. 7 – Ligand binding region of rat Mrp2 estimated by in silico study. Ligand binding region of rat Mrp2 was estimated by using the three-dimensional (3D) pharmacophore (key functional groups of ligand molecules) of multiple substrates of this transporter and the method of quantitative structure–activity relationship (3D-QSAR) comparative molecular-field analysis (CoMFA). This method revealed a primary binding region, including two hydrophobic and two electrostatically positive sites, and a secondary binding region, including two electrically positive and two electrostatically negative sites, which is attributable to a broad substrate specificity of rat Mrp2 (Hirono et al., 2005).

structure–activity relationship analysis. From this analysis, they estimated the ligand binding region of rat Mrp2 (Fig. 7) including two hydrophobic and two electrostatically positive sites (primary binding sites). In addition, they estimated secondary binding sites including two electrostatically positive and two electrostatically negative sites, which attribute to a broad substrate specificity of rat Mrp2.

3. The mechanism of transporter-mediated drug–drug interactions

We analyzed the mechanism of the drug–drug interaction between cerivastatin and CsA and showed that CsA inhibited the transporter (including OATP1B1)-mediated uptake with only a minimal effect on the microsomal metabolism, suggesting that this drug–drug interaction is due to the transporter-mediated uptake process (Shitara et al., 2003). The pharmacokinetics of cerivastatin is also affected by the coadministration of gemfibrozil (Backman et al., 2002). This is due to inhibition of the microsomal metabolism by gemfibrozil glucuronide (Shitara et al., 2004b). It should be noted that CsA, a transporter inhibitor, alters the AUC with only a minimal effect on the elimination half-life ($t_{1/2}$) while gemfibrozil, a metabolic inhibitor, increased both of the AUC and $t_{1/2}$ (Muck et al., 1999; Backman et al., 2002; Shitara et al., 2005). This can be explained as follows. The $t_{1/2}$ can be described by the following equation using CL_{tot} and distribution volume (V_d).

$$t_{1/2} = \frac{\ln 2 \cdot V_d}{CL_{tot}} \quad (6)$$

Cerivastatin is highly distributed to the liver, due to the efficient transporter-mediated hepatic uptake and extensive protein binding in the liver, and the V_d mainly depends on the distribution to the liver. For this drug, inhibition of the transporter-mediated hepatic uptake leads to a reduction in V_d. Transporter-mediated hepatic uptake is also a determinant of its hepatic clearance. Thus, CsA simultaneously reduces V_d and CL_{tot} to similar levels, resulting in no alteration in $t_{1/2}$. On the other hand, gemfibrozil inhibits the metabolism with only a minor effect on the transporter-mediated hepatic uptake of cerivastatin. Thus, it reduces the CL_{tot} but does not change the V_d so much, leading to a prolongation of $t_{1/2}$. The pharmacokinetics of bosentan was reported to be changed by coadministration of CsA in rats and humans (Binet et al., 2000; Treiber et al., 2004). It is also due to inhibition of the transporter-mediated hepatic uptake as described above (Fig. 3(A)). The plasma concentration of repaglinide is also altered by coadministration of CsA in humans (Kajosaari et al., 2005). This interaction is, at least partly, caused by the inhibition of OATP1B1-mediated hepatic uptake. The extent of the alteration caused by this interaction was significantly lower in patients with a genetic polymorphism in OATP1B1 (T521C), suggesting the involvement of OATP1B1-mediated hepatic uptake in this interaction (Kajosaari et al., 2005).

Transporter-mediated drug–drug interactions can occur in the biliary excretion process as well as the uptake process. Ueda et al. described a method to quantitatively predict the pharmacokinetic alteration caused by a drug–drug interaction, considering the inhibition of biliary excretion as well as uptake (Ueda et al., 2001). They examined the effect of probenecid on the uptake of methotrexate in isolated rat hepatocytes and rat bile canalicular membrane vesicles to determine the inhibition constants (K_i) of probenecid for the purpose of a quantitative prediction of the extent of drug–drug interaction between these two drugs in vivo from the in vitro studies (Fig. 8(A)). They also examined the inhibitory effect of probenecid on the in vivo biliary excretion of methotrexate, which is excreted in the bile in rats, to validate their prediction (Fig. 8(A)). The uptake of methotrexate by isolated rat hepatocytes and bile canalicular membrane vesicles were inhibited by probenecid with K_i of 180 and 52 μM, respectively. Probenecid also reduced the biliary excretion clearance in rats in vivo in a concentration-dependent manner. Although the degree of the reduction in the hepatic uptake and biliary excretion are well predicted by the reduction in the uptake in isolated hepatocytes and bile canalicular membrane vesicles, the degree of the reduction in the net clearance is found to be overestimated by a simple calculation of the product of the reduction in the hepatic uptake and biliary excretion (Fig. 8(B)–(D)). This suggests that the actual degree of the drug–drug interaction should be estimated considering that the hepatic clearance ranges between Eqs. (2) and (3) described in Section 2.2.

Matsushita et al. examined the effect of benzylpenicillin on the pharmacokinetics of cefodizime in rats (Matsushita et

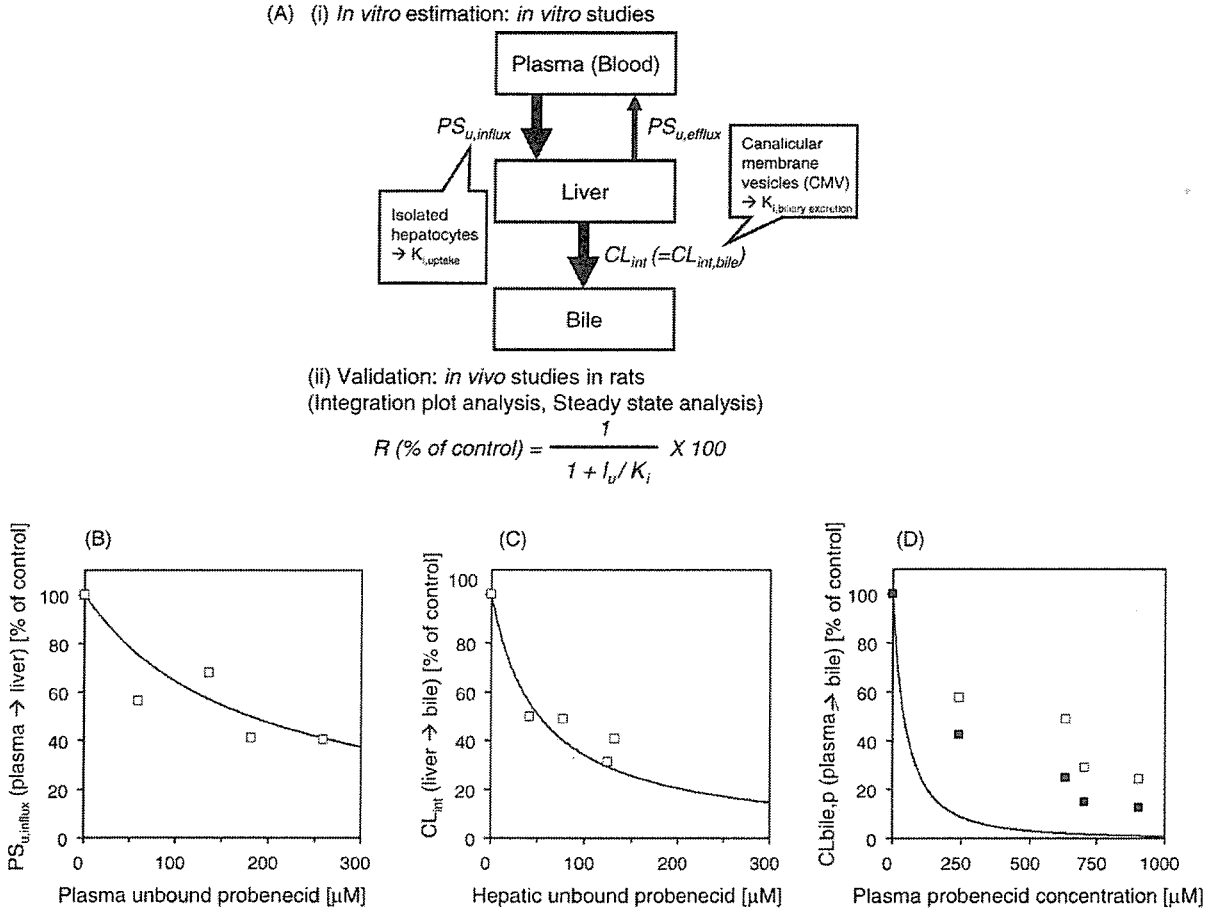

Fig. 8 – Extrapolation of the drug interaction between methotrexate and probenecid in the process of transport across the sinusoidal and canalicular membrane, and the net biliary excretion from in vitro data. For the in vitro to in vivo extrapolation of transporter-mediated drug–drug interaction between methotrexate (MTX) and probenecid (PBN) in the process of biliary excretion, the inhibitory effect of PBN on the uptake of MTX into isolated rat hepatocytes and bile canalicular membrane vesicles was examined by in vitro studies. The results obtained in these studies were extrapolated to in vivo to predict the in vivo drug–drug interaction. This extrapolation was validated by the comparison with the pharmacokinetic alterations observed in vivo. The reduction in the hepatic uptake of unbound MTX across the sinusoidal membrane ($PS_{u,influx}$) by PBN was extrapolated from in vitro data (—) based on the inhibition constant (K_i) for the uptake of MTX into isolated rat hepatocytes and inhibitor unbound concentration in vivo (I_u) by $(1/(1 + I_u/K_i)) \times 100$ [% of control] (B). This prediction was well matched with the observed value in vivo (□). The reduction of the biliary excretion was also predicted using in vitro data based on the K_i for the uptake of MTX into rat bile canalicular membrane vesicles and I_u and shown in (C). The reduction in the net biliary excretion of MTX was also predicted by the simple calculation of the product of the reduction in the hepatic uptake and biliary excretion (D). The predicted values based on inhibitor unbound concentration in the plasma (—) and in the liver (■) are shown. This simple prediction resulted in an overestimation of the reduction of the net biliary excretion compared with the observed value (□) (Ueda et al., 2001).

al., 1992). Cefodizime undergoes biliary excretion in the liver and glomerular filtration in the kidney. Therefore, the CL_{tot} of cefodizime can be described by the following equation.

$$CL_{tot} = CL_H + CL_R = CL_H + f_B\,GFR \quad (7)$$

where f_B and GFR are the blood protein unbound fraction and the glomerular filtration rate, respectively. Coadministration of benzylpenicillin apparently had no effect on the pharmacokinetics of cefodizime. However, benzylpenicillin reduced the hepatobiliary transport of cefodizime, resulting in a reduction in hepatobiliary clearance. In addition, benzylpenicillin reduced its plasma protein binding, leading to an increased renal clearance (Fig. 9). The reduced hepatobiliary excretion and increased urinary excretion resulted in no alteration in the plasma concentration of cefodizime. It is, thus, possible that drug–drug interaction might not be revealed by measuring only the plasma concentration profile.

Although renal excretion of famotidine is affected by coadministration of probenecid in humans, it is not altered in rats, suggesting there is an inter-species difference in the renal clearance mechanism of famotidine (Lin et al., 1988; Inotsume

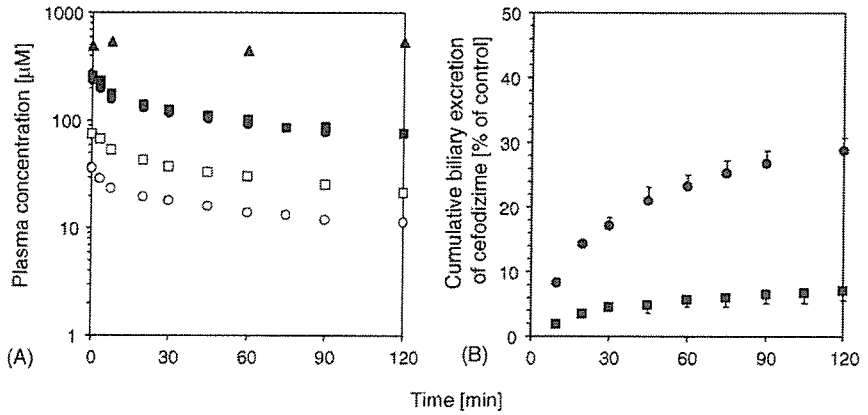

Fig. 9 – Effect of benzylpenicillin on the disposition of cefodizime. Data are taken from the result by Matsushita et al. (A) (▲) plasma concentration of benzylpenicillin; (■, ●) plasma concentration of cefodizime with or without coadministration of benzylpenicillin, respectively; (□, ○) plasma unbound concentration of cefodizime with or without coadministration of benzylpenicillin, respectively. (B) Coadministration of benzylpenicillin does not affect the plasma concentration of cefodizime (A). However, benzylpenicillin reduces the biliary excretion. On the other hand, it increases the plasma protein unbound fraction, resulting in the enhanced urinary excretion. Reduced hepatic clearance and increased renal clearance resulted in no apparent alteration in the disposition of cefodizime (■ and ●) (Matsushita et al., 1992).

et al., 1990) (Fig. 10(A)). Tahara et al. examined the effect of probenecid on the uptake of famotidine by renal transporters in order to clarify the mechanism of this inter-species difference (Tahara et al., 2005a). H_2 receptor antagonists are reported to be substrates of solute carrier 22 (SLC22) family transporters including OCTs and OATs. Tahara et al. examined the uptake of H_2 receptor antagonists in human and rat OAT and OCT family transporters and the inhibitory effects produced by other drugs (Tahara et al., 2005a). They analyzed the inter-species differences and found that the transport activity of famotidine by rat Oat3 was not as high as that by human OAT3. In humans, the inhibition of the OAT3-mediated transport of famotidine by probenecid caused a drug–drug interaction. However, in rats, this inhibition does not cause a marked interaction, possibly due to the smaller contribution made by Oat3 to the renal clearance in rats. In addition, Oct1 as well as Oct2 (*Slc22a2*) accepts famotidine as a substrate and possibly contributes to the renal clearance of famotidine in rats while, in humans, OCT1 (SLC22A1) is not expressed in the kidney. Probenecid does not interact with OCTs. Thus, the inter-species difference, exhibited by the fact that probenecid alters the pharmacokinetics of famotidine in humans but not in rats, is caused by an inter-species difference in the activities of the OAT3/Oat3-mediated transport of famotidine and the existence of Oct1 in rat kidney (Fig. 10(B)). Tahara et al. also examined inter-species differences in the transport activities of OAT1/Oat1 and OAT3/Oat3 in humans, rats and monkeys, using different substrates (Tahara et al., 2005b). A good correlation was observed in the case of humans versus rats and humans versus monkeys as far as OAT1/Oat1-mediated transport was concerned (Fig. 11). However, in the case of OAT3/Oat3-mediated transport, a good correlation was observed in the case of humans versus monkeys, while a relatively poor correlation was observed in the case of humans versus rats (Fig. 11). This suggests that an extrapolation from rat to human data is not necessarily appropriate for OAT3 substrates.

More recently, Tahara et al. examined the effect of probenecid on the pharmacokinetics of famotidine in monkeys in vivo (Tahara et al., in press). In monkeys, probenecid caused a 65% reduction in the renal clearance and a 90% reduction in the tubular secretion, which is very similar to the corresponding interaction observed in humans. In addition, they showed the absence of Oct1 in monkey kidney. This result also supports the belief that the monkey is more appropriate animal model for predicting OAT3-mediated drug–drug interactions involving renal excretion in humans.

4. A method for estimating the contribution of each transporter to the total hepatic uptake

4.1. *The importance of the contribution of transporters*

Currently, great progress is being made in the molecular cloning of transporters. These studies help to characterize the molecular mechanisms of drug transport by using transporter-expressing systems. However, the contribution of each transporter to drug transport in vivo has not yet been evaluated. Using these contributions, the uptake clearance in the transporter-expressing systems can be extrapolated to that in the tissue, and it is possible to quantitatively predict the transporter-mediated drug–drug interactions and pharmacokinetic alterations in humans with single nucleotide polymorphisms (SNPs) in their transporter(s), in specific pathophysiological disorders and so on. In this section, the estimation of the transporter contributions is described.

4.2. *Estimation of the contributions of specific transporters to the total hepatic uptake*

Studies to characterize the contributions of transporters to the total hepatic uptake have been performed. For example, Hagenbuch et al. used the method to estimate the contri-

(A) Rat

	CL_{renal} [mL/min/kg]
Famotidine alone	42.3 ± 8.9
with probenecid	45.8 ± 10.3

Human

	CL_{renal} [mL/min]	$CL_{secretion}$ [mL/min]
Famotidine alone	297 ± 19	196 ± 21
with probenecid	107 ± 5	22.0 ± 4.2

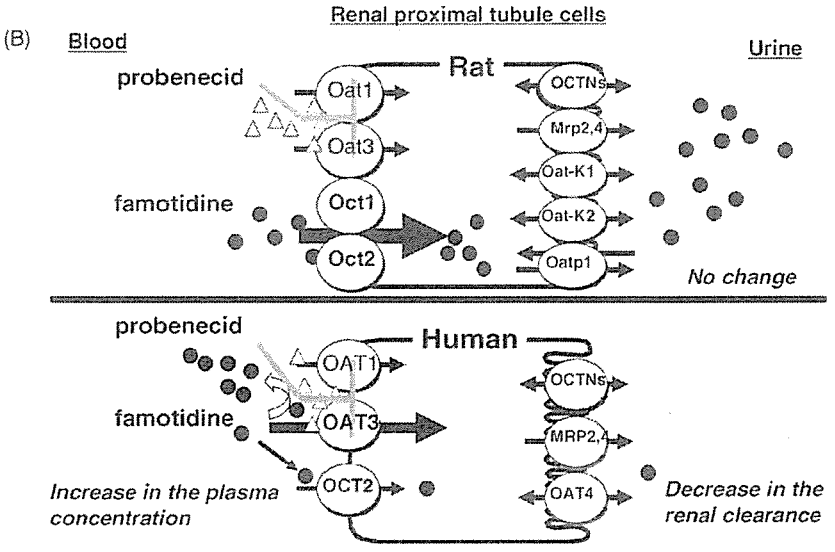

Fig. 10 – Inter-species difference between rats and humans in the drug–drug interaction between famotidine and probenecid. (A) Probenecid does not alter the renal clearance of famotidine in rats while it decreases that in humans (Inotsume et al., 1990; Lin et al., 1988). (B) This inter-species difference can be explained by the different mechanism of renal excretion of famotidine in rats and humans. The contribution made by Oat3 to the uptake of famotidine across the basolateral membrane in renal epithelial cells in rats is smaller than that in humans. In rats, Oct1 exists in the kidney and it contributes to the renal uptake of famotidine. In humans, OAT3-mediated transport of famotidine is inhibited by probenecid while, in rats, Oct1-mediated transport is not inhibited and Oat3-mediated transport is minor. Thus, the renal secretion of famotidine is affected by the coadministration of probenecid in humans but not in rats.

bution of specific transporters by coinjecting antisense DNA to this transporter with total mRNA isolated from rat liver into *Xenopus laevis* oocytes (Hagenbuch et al., 1996). They estimated the contributions of Na^+-taurocholate cotransporting polypeptide (Ntcp; *Slc10a1*) and Oatp1a1 to the uptake of taurocholate (TC) and bromosulfophthalein (BSP) by this method. In their report, they revealed that the Na^+-dependent and Na^+-independent uptakes of TC are mostly mediated by Ntcp and Oatp1a1, respectively. They also revealed that only half of the uptake of BSP attributes to Oatp1a1, suggesting an existence of other transporter(s) responsible for its uptake. In fact, as of now, other transporting systems than Oatp1a1, which include Oatp1b2, has been reported (Cattori et al., 2000). Nakai et al. applied this method to examine the contribution of human OATP1B1 to the hepatic uptake of pravastatin and estradiol 17β-D-glucuronide ($E_2$17βG) (Nakai et al., 2001). They have shown that microinjection of cRNA for human OATP1B1 and human liver polyadenylated RNA into *Xenopus laevis* oocytes enhanced the uptake of pravastatin and $E_2$17βG and coinjection of antisense DNA for human OATP1B1 with human liver polyadenylated RNA resulted in a decrease of the uptake of these compounds to the similar level with that in water-injected oocytes. They concluded that OATP1B1 mainly contributes to the hepatic uptake of them. As of now, as many